African Railway Center of Excellence

Addis Ababa Institute of Technology

MSc Railway Engineering (Civil Infrastructure)

INVESTIGATION OF BALLAST DEGRADATION ON ETHIO-DJIBOUTI RAILWAY LINE IN ETHIOPIA

A thesis submitted to the African Railway Center of Excellence (ARCE) in partial fulfillment of the requirements for the Addis Ababa Institute of Technology's Masters of Science in Railway Engineering (Civil Infrastructure)

By:

SAKINA MRINA JUMA

GSR/3098/12

Advisor: Dr. Tensay Gebremedhin

October 2021

Addis Ababa

Ethiopia

APPROVAL PAGE

The undersigned have examined the thesis entitled "***Investigation of Ballast Degradation on Adama-Miesso Railway Line in Ethiopia***" presented by Sakina Mrina Juma (GSR/3098/12), submitted to African Railway Center of Excellence, Addis Ababa Institute of Technology, School of Graduate Studies in partial fulfillment of the requirement of the award of Degree of Masters of Science in Railway Engineering (Civil Infrastructure).

Submitted by:

Sakina Mrina Juma

Student	Signature	Date

Approved by:

Dr.Tensay Gebremedhin
Assistant Professor

Advisor	Signature	Date

Dr. Henok Fikre Gebregziabher
Assistant Professor

Examiner	Signature	Date

Mr. Anteneh Zewdu
External Examiner

Examiner	Signature	Date

Dr. Abrham Gebre
Associate Professor

Director of ARCE	Signature	Date

DECLARATION

This is to declare that the work presented here in this thesis with the title **"*Investigation Of Ballast Degradation On Adama-Miesso Railway Line in Ethiopia*"** is original, has not been presented for a degree of any other university and all the resource of materials used for this thesis have been suitably cited.

_____ _____

Sakina Mrina Juma Date

ACKNOWLEDGMENT

Firstly, my gratitudes go to Allah for giving me the opportunities to accomplish this milestone. None but Him alone is the Most Merciful.

Also, I will like to express my appreciation to my family for their prayers, moral, and financial supports to achieve this feat. Surely, family is everything.

Moreover, my appreciation to the National Institute of Technology for the funding to pursue my MSc Program in Civil Infrastructure Engineering. In addition, my appreciations go to the staff of the Ethiopian Railway Cooperation for their supports during the data acquisition for this study.

Finally, my deepest appreciation to my Advisor, Dr. Tensay Gebremedhin, Senior Scientist of Geotechnical Engineering, School of Civil and Environmental Engineering, Addis Ababa Institute of Technology for his guidance and support throughout this study. Again, my appreciations go to Mr. Ayele, and Mr. Tedrowos for their assistance, especially during data and sample collections.

ABSTRACT

Ballasted tracks are widely used due to their low construction costs, availability of materials, and ease of maintenance. The ballast layer provides resiliency to cyclic loads, drainage, and space for fines accumulation. The primary issue with ballasted tracks is their progressive degradation over time and use. Ballast degradation weakens the interlocking of particles, resulting in insufficient bearing capacity, differential settlements in rail tracks, and obstructing the free drainage of the ballast layer. Understanding the extent to which the ballast bed degrades under cyclic loading enables either standardization or the planning of maintenance schedules.

This study was conducted to determine the extent of ballast degradation along the Adama-Miesso section of the Ethiopia-Djibouti railway line following three years of operation. This study collects data on ballast degradation through visual inspections in the field and laboratory tests. Visual inspections were conducted following the severity ranking criteria, which place a premium on the presence of vegetation growth within the ballast. On samples of ballast collected from eight locations along the Adama-Miesso sections, laboratory tests including grading, Los Angeles Abrasion, shape tests (Elongation and Flackiness), specific gravity and absorption, Aggregate Impact Value, and Aggregate Crushing Value were conducted. Gradation was determined by calculating the percentage shift of each PSD curve from the as-built PSD curve limits, as well as Marsal's breakage indices and the material finer than 0.075mm standard sieve size at each location. Additionally, AREMA gradations were compared to the gradations at each location. Mechanical and physical characteristics of the ballast were compared to those of various railway ballast standards. Using Alyamani and Sen's empirical formula, the permeability of the ballast was determined.

The investigation discovered that the ballast on the Adama-Miesso section had degraded significantly over three years of operation, necessitating maintenance.

Keywords: Ballast; Degradation; Investigation; Railway line; Laboratory tests; Field Inspections.

LIST OF ACRONYMS

AASHTO	American Association of State Highway and Transportation Officials
ACV	Aggregate Crushing Value
AIV	Aggregate Impact Value
AREMA	American Railway Engineering and Maintenance-of-Way Association
AS	Australian Standard
ASTM	American Society for Testing and Materials
B	Breakage ratio
BAp	BBP
BBp	Ballast Breakage percentage
BBI	Ballast Breakage Index
Bg	Marsal's breakage
Bp	Breakage potential
Br	Relative Breakage
BR	British Rail
BS	British Standard
Bt	Total breakage
Cc	Coefficient of Curvature
Cu	Coefficient of Uniformity
EI	Elongation Index

EN	European Standard
FI	Flakiness Index
FI	Fouling index
k	Permeability
LAAV	Los Angeles Abrasion Value
NSC	Norfolk Southern Corporation,
P<0.075mm	Particles finer than 0.075mm standard sieve
PSD	Particle Size Distribution
S.G	Specific Gravity
Wasb	Water Absorption

LIST OF FIGURES

Figure 1: Map of the Study Area showing Route Alignment 1
Figure 2: Cross Section of Ballasted Track [10]. 3
Figure 3: Proposed Parent Rock Classification for Selection of Ballast Aggregate [7] 6
Figure 4: Schematic of Ballast Zones in Railway Track, (a) Cross-section, (b) Plan and, (c) Longitudinal Section. 7
Figure 5: Flakiness index gauge 11
Figure 6: Elongation index gauge 12
Figure 7: AREMA #24 and #4 ballast gradation particle size ranges 19
Figure 8: PSD of modified AREMA No 3 used by NSC 21
Figure 9: Critical ballast fouling phases [12] 22
Figure 10: Definition of Breakage Potential (Bp) [20]. 24
Figure 11: Definition of Total Breakage (Bt) [20]. 24
Figure 12: Definition of Ballast Breakage Index (BBI) [16]. 25
Figure 13: Definition of Breakage Index, B. 26
Figure 14: The section along Adama-Miesso at K 229+207 with mud plain, and vegetations 36
Figure 15: The section along Adama-Miesso at K210+ 626 with surface fines and high degraded ballast. 37
Figure 16: The section along Adama-Miesso at K274+810 with missing shoulder ballast 37
Figure 17: The section along with Adama-Miesso at K314+529 heaved shoulders and cobles on the main track. 38
Figure 18: PSD curves with percentage passing above the as-built maximum value 39
Figure 19: PSD curves with percentage passing below the as-built minimum value 39
Figure 20: PSD Curves compared with the as-built limits 40
Figure 21: Ballast Breakage Index (Bg) of aggregates along Adama-Miesso Section 41
Figure 22: Coefficient of Uniformity Cu, and Permeability Factor, kf/ki of ballast 42
Figure 23: Comparison of PSD curves of ballast aggregates with AREMA gradations 46
Figure 24: Mechanical properties of the ballast aggregates and recommended maximum limits 48
Figure 25: A Clustered Bar Chart Showing the Shape Properties of the Ballast at Different Locations 48
Figure 26: A Clustered Bar Chart Showing the Physical Properties of the Ballast at Different Locations 50
Figure 27: PSD curves of as-built compared with the design limits 56
Figure 28: PSD curve at K112+800 section compared with the as-built limits 56
Figure 29: PSD curve at chainage K146+820 compared with the as-built limits 56
Figure 30: PSD curve at chainage K251+480 compared with the as-built limits 57
Figure 31: PSD Curves at Chainage K327+000 Compared with the as-built limits 57
Figure 32: Test methods for mechanical and physical properties 61

LIST OF TABLES

Table 1: Contribution of ballast portions to perform ballast duties 7
Table 2: Recommended limiting value for ballast materials quality (AREMA 2007) [12] 13
Table 3: Track ballast layer specification indices 14
Table 4: Track ballast assessment based on the proposed categorization of ballast technical requirement 16
Table 5: Recommended AREMA ballast gradings (after AREMA, 2000) 20
Table 6: Modified AREMA No.3 grading (after Norfolk Southern Corporation, 2011) 20
Table 7: State of ballast degradation based on FI according to Selig and Waters,1994 [24] 26
Table 8: Test sample sizes for aggregate gradation test 30
Table 9: Gradings of Test Samples 31
Table 10: Number of abrasive charges for above samples 32
Table 11: Minimum mass of test portion 32
Table 12: Data for Determination of Flakiness Index 33
Table 13: Data for Determination of Elongation Index 33
Table 14: Percentage (%) shift of PSD curves from the as-built values 40
Table 15: Gradations and observations from different locations 42
Table 16: Ballast mechanical properties and the recommended values in standards 47
Table 17: Ballast physical properties and the AREMA recommended values 49
Table 18:Summary of ballast properties degradation at the selected locations 50
Table 19: As-Built Parametric Values and Standard Specification Values 57
Table 20: Current Insitu Ballast Aggregate Gradations 58
Table 21: Calculation of Marsal Breakage ratio, B_g. 58
Table 22: Ballast aggregates characteristics; D_{10}, D_{30}, D_{50}, D_{60}, k, k_f/k_i, C_u, and C_c 59

TABLE OF CONTENTS

APPROVAL PAGE i
DECLARATION ii
ACKNOWLEDGMENT iii
ABSTRACT iv
LIST OF ACRONYMS v
LIST OF FIGURES vii
LIST OF TABLES viii
TABLE OF CONTENTS ix
1. INTRODUCTION 1
1.1. Problem Statement 3
1.2. Objective 3
1.2.1. General Objective 3
1.2.2. Specific Objectives 3
1.3. Research Questions 4
1.4. Significance of the Research. 4
1.5. Scope and Limitations of the Research. 4
2. LITERATURE REVIEW 5
2.1. Ballast 5
2.1.1. Ballast Functions 6
2.1.2. Ballast Portions 6
2.2. Ballast Assessment 8
2.2.1 Load resistant characterization 8
2.2.2 Assessment of Stability Properties 10
2.2.3 Assessment of weathering 12
2.2.4 Cementing characteristics of ballast 14
2.3. Gradation(Particle Size Distribution) 18
2.3.1.American ballast specification 19
2.4. Ballast Degradation Mechanisms. 21
2.4.1.Ballast fouling 21
2.5. Quantification of Ballast Particle Breakage 23

2.6. Permeability of Ballast 27
3. MATERIALS AND METHODOLOGY 28
3.1. Literature review 28
3.2. Field Investigation 29
3.3. Samples and sampling procedures 29
3.3.1.Sampling according to AASHTO R 90 29
3.3.2.Reducing Samples to Test Size according to ASTM C702 [30] 29
3.4. Material Testing 30
3.4.1.Gradation (Sieve Analysis)According to ASTM C117 and C136 [31]and [32]. 30
3.4.2. Los Angeles Abrasion according to ASTM C535 [33] 30
3.4.3.Flakiness Index According to BS812:1989 [34]. 32
3.4.4.Elongation Index According to BS812:1990 [34]. 33
3.4.5.Aggregate Impact Value according to BS 812-112:1990 [33] 34
3.4.6.Aggregate Crushing Value (ACV) according to BS 812-110:1990 [33] 34
3.4.7.Specific Gravity and Absorption of Aggregates according to BS812:Part 2:1975[35] 35
4. RESULTS AND DISCUSSIONS 36
4.1. Field Investigation 36
4.2. Ballast Gradation 38
4.3. Ballast Properties 46
4.3.1 Ballast Mechanical Properties 46
4.3.2. Ballast Shape Properties 48
4.3.3 Ballast Physical Properties 49
4.4. Summary of Result Findings 50
4.5. Conclusions 51
4.6. Recommendations 52
References 53
Appendices 56

1. INTRODUCTION

The Ethio-Djibouti Railway Line is an electrified, ballasted, standard gauge track of a total length of 756 km with 45 stations. It is the first modernized railway track in East Africa that connects Ethiopia´s capital, Addis Ababa, and the Port of Djibouti, which is the major hub for the Gulf of Aden. The line is a Class II track, composed of mixed traffic operating at a velocity of 120 km/h and 80 km/h for passenger and freight respectively. Adama-Miesso section is a single line track with total a length of 215.34 km. Figure 1 shows the map of the study area.

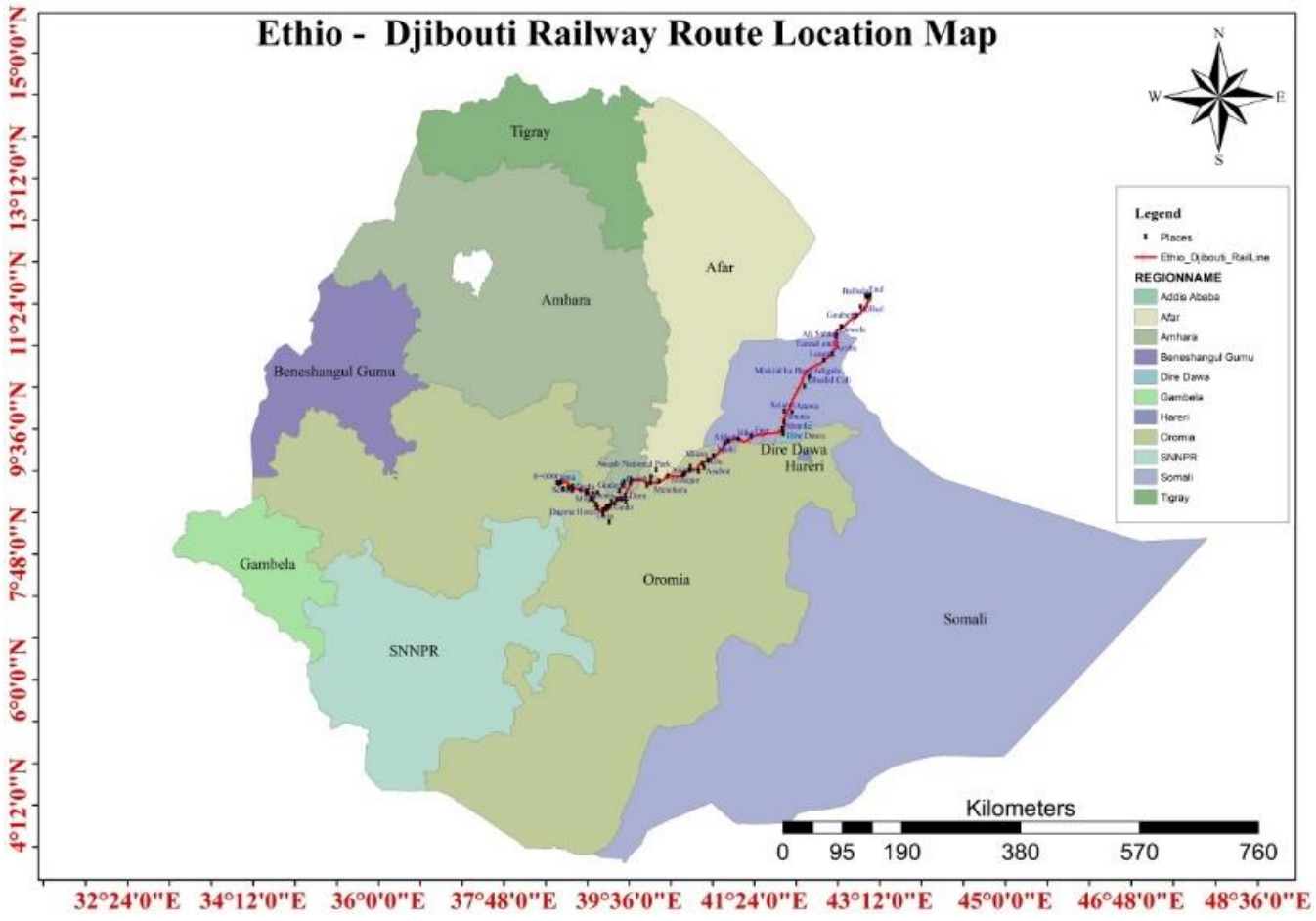


Figure 1: Map of the Study Area showing Route Alignment

Railroads are a low-energy mode of transport that comprise the world's largest network, providing rapid and secure public and freight transportation. Ballasted tracks, which consist of a ballast layer sandwiched between sleepers and a sub ballast layer, are the most widely used railway tracks worldwide [1]. A rail track's structure is classified into two types: substructure and superstructure (Figure 2). The superstructure is composed of tracks, a fastening system, and sleepers, while the substructure is composed of a ballast

layer, a sub ballast layer, and a subgrade. However, in many parts of Europe, the ballast may be considered to be a component of the superstructure [2]. Ballast is a critical component of the traditional track system, and its importance has grown in recent years as axle weights and train speeds increased [3]. The ballast should perform the following functions: to resist vertical, horizontal, and lateral forces[4] from the base of sleepers, provide track elasticity and pressure reduction, ensure effective drainage of water, and allow for vertical and horizontal alignment defects correction [5]. The ballast layer's primary functions are to distribute stresses caused by train loading, to provide lateral resistance, and to facilitate railway drainage [6].

To perform satisfactorily the functions outlined above, ballast must exhibit certain characteristics, including particle size, shape, gradation, surface roughness, particle density, bulk density, strength, durability, hardness, toughness, and resistance to attrition and weathering [3]. Railway industries face challenges in terms of increasing efficiency and lowering maintenance and infrastructure costs as a result of growing demand for public and freight transport.

A common issue with this section of track is the premature degradation of ballast due to increased traffic passage, loads, and speed, which results in the loss of high track quality, necessitating maintenance work and resulting in high maintenance and downtime costs [7]. Ballast degradation erodes the interlocking between particles, resulting in insufficient bearing capacity, differential settlements in rail tracks, and obstructing the free drainage of the ballast layer [8]. Worldwide, significant funding is committed in railway maintenance, with a significant percentage of this funding going toward geotechnical issues with substructure layers, including the ballast layer [9]. Railway authorities in the United States of America spend tens of millions of dollars annually on ballast and related maintenance costs, while Canadian railroads reported spending approximately one billion dollars annually on the procurement, distribution, and rehabilitation of ballast, which accounts for up to 40% of their track replacement and upkeep costs [9]. To minimize these expenditures, it is critical to conduct a detailed investigation of the ballast's behavior under load and the track's environmental conditions.

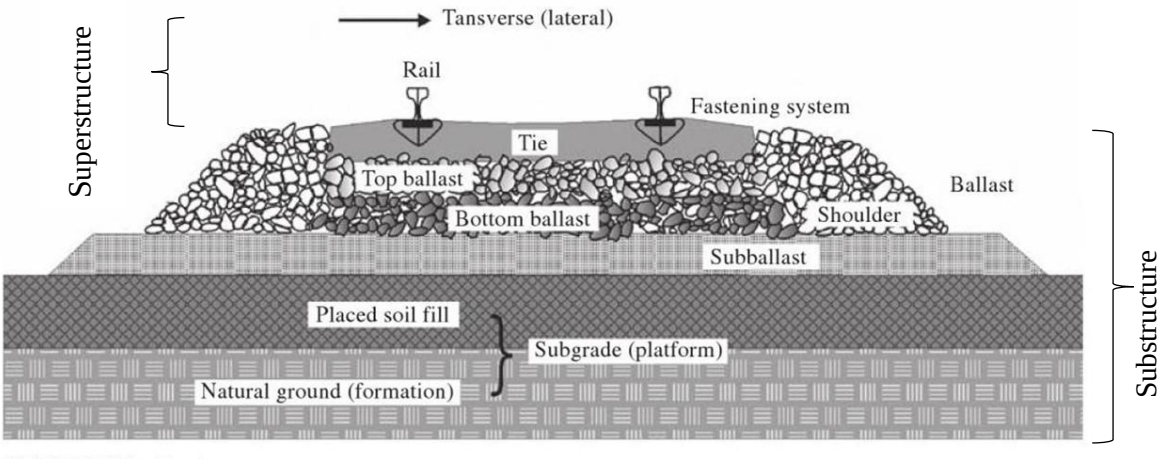


Figure 2: Cross Section of Ballasted Track [10].

1.1. Problem Statement

A typical issue with conventional railway tracks is the gradual degradation of ballast as traffic volume increases (number of load cycles). Numerous field and laboratory studies were undertaken in North America have indicated that track fouling is mostly caused by ballast breakage [3]. Ballast fouling is caused by 76 percent, 1%, 7%, and 3% of ballast degradation, sleeper, surface, underplaying granular layer, and subgrade, correspondingly [5]. Increased transportation demands result in increased traffic load and running speed on the track, which inevitably results in faster degradation of the ballast material and an increase in track geometry loss. A more precise assessment of ballast conditions enables the identification of dawns associated with unsafe track support conditions and the development of effective maintenance plans [11]. From an economic standpoint, the life cycle costs of ballast are determined by the cost of maintenance work such as tamping and ballast cleaning that is required to maintain service quality. A thorough understanding of ballast qualities and the performance of appropriate tests are prerequisites to lowering maintenance costs [7]. Routine maintenance is critical in a ballasted track to maintain the intended safety level, design speed, and passenger comfort.

1.2. Objective

1.2.1. General Objective

The General objective of the study is to investigate ballast degradation on Adama-Miesso Railway Line.

1.2.2. Specific Objectives

The Specific objectives of the study are:

- Assessment of ballast bed degradation on the field through visual inspections.
- Ballast quality assessment through laboratory investigations.
- Study of ballast quality degradation trend.
- Comparison of present ballast quality with various railway ballast specifications

1.3. Research Questions

- What is the current quality of the ballast on Adama- Miesso Railway Line?
- Is the existing quality acceptable or need for maintenance/replacement?

1.4. Significance of the Research.

The ballast layer is critical and the largest component of the track, including more than 1600 m3 and 2500 metric tons of material by volume and weight for a single kilometer of track [7]. The ballast bed volume is approximately 2407 m^3 per kilometer for the Adama-Miesso segment. With time and usage, the ballast bed degrades gradually. Proper ballast selection and manufacturing ensure a low degradation rate, resulting in a longer ballast life and fewer maintenance cycles. Because railway systems require significant investment, preventative and routine maintenance is critical to ensure their lifespan. Investigating ballast degradation enables a determination of whether the ballast should be maintained or replaced to prolong the track's life and ensure safe riding.

1.5. Scope and Limitations of the Research.

The case study for this research is the Adama-Miesso section with a length of 215.45km. Only eight samples were used in this study due to time constraints and accessibility. Because ballast degrades with usage and time then the results are only valid to represent the condition of ballast degradation at the time of sample collection which was April 2021.

2. LITERATURE REVIEW

2.1. Ballast

Ballast is defined as selected crushed granular aggregates ranging in size from 10 to 60 millimeters that are placed as the top layer of the substructure, typically 250 to 350 millimeters, in which sleepers are implanted to hold the rails [10]. The Ballast is a key structural part of the railroad and its main function is to transfer the induced loads from the superstructure to the subgrade without failure and provide good drainage. Ballast is ideally composed of coarse aggregates sourced from either blasted igneous rock, metamorphic or, well-cemented sedimentary rock quarries [12]. The aggregates that often fail to perform as ballast would include various types of sandstones mainly because of softening upon wetting and the inability to withstand high cyclic loads [3]. Although blast furnace slag can be used as ballast, its load-carrying capability is inferior to that of freshly quarried natural rock aggregates. A good ballast should be firm, strong, and stable, as well as workable, drain easily, easy to clean and re-clean, and resistant to deformation under weight. Historically, aggregates possessing the following characteristics have been regarded as the optimal ballast material [13].

- Angular, crushed,
- Hard stones and rock
- Uniformly graded
- Free of dust, dirt, and resistance to cementing action

External influences must be resisted with ballast. Extreme cyclic loads, fluctuating frequency and intensity vibrations, frequent wetting and drying leading to crystallization of rain-dissolved soluble salts, and other variables all contribute to the ballast's degraded condition. Additionally, ballast must be easy to handle during maintenance [14].

The ballast used to support railway tracks is critical in developing and sustaining the track response characteristics and, consequently, the riding quality. For ballasted tracks, the primary criterion for low maintenance expenditures is an elastic, non-cemented, stable, and weather-resistant ballast bed that is adequately laid and compacted on a stable, compact sub-ballast and subgrade [14]. The proposed parent rock classification to select ballast aggregate is depicted in Figure 3.

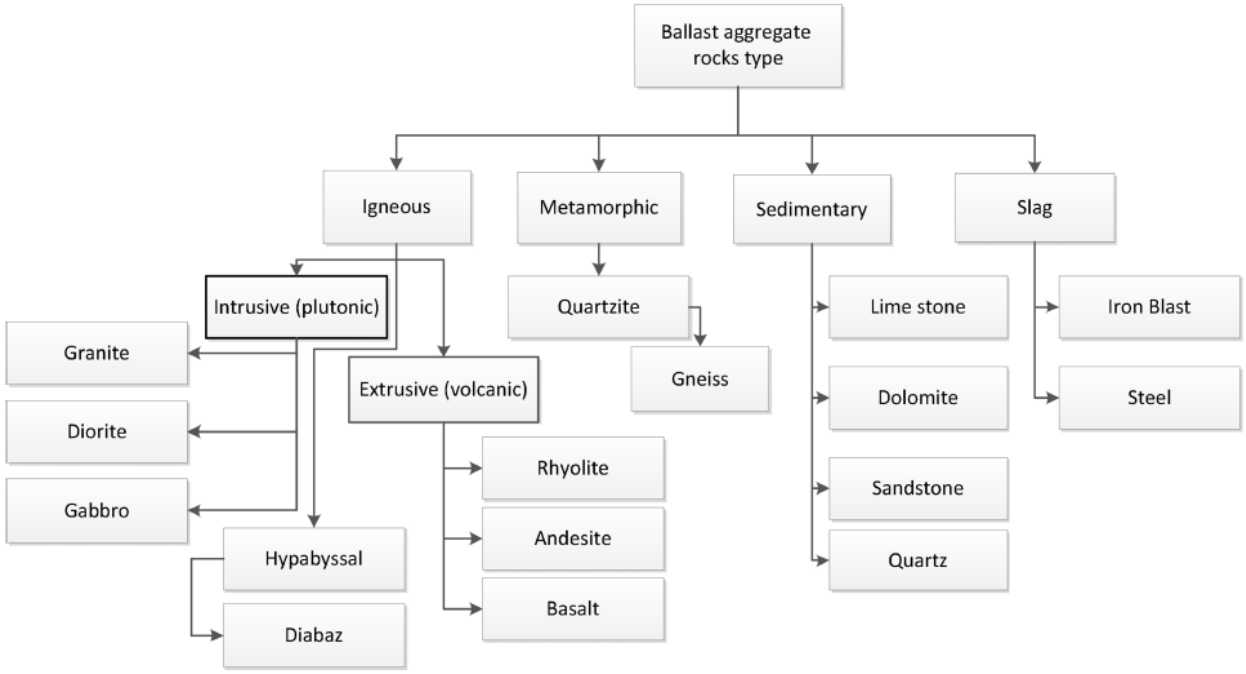


Figure 3: Proposed Parent Rock Classification for Selection of Ballast Aggregate [7]

2.1.1. Ballast Functions

The ballast should perform the following functions [3]

i) withstand external loads to maintain track position.
ii) ensure effective water drainage.
iii) make track surfacing and alignment maintenance more convenient.
iv) give the necessary robustness to absorb huge and dynamic loads.
v) give sufficient void space for the storage of ballast fines without interfering with the interaction of ballast particles
vi) prevent weed development by minimizing fouling
vii) absorb noise and provide sufficient electrical resistance

2.1.2.Ballast Portions

The ballast aggregate is laid above the sub-ballast layer, between the sleepers (crib), and beyond the sleeper ends (shoulder) [7] as shown in Figure 4.

i) **Crib ballast**. Crib ballast is the ballast located between the sleepers. The crib ballast provides pressure on the ballast below the sleepers, increasing the stability of the track and preventing longitudinal movement of the sleepers.

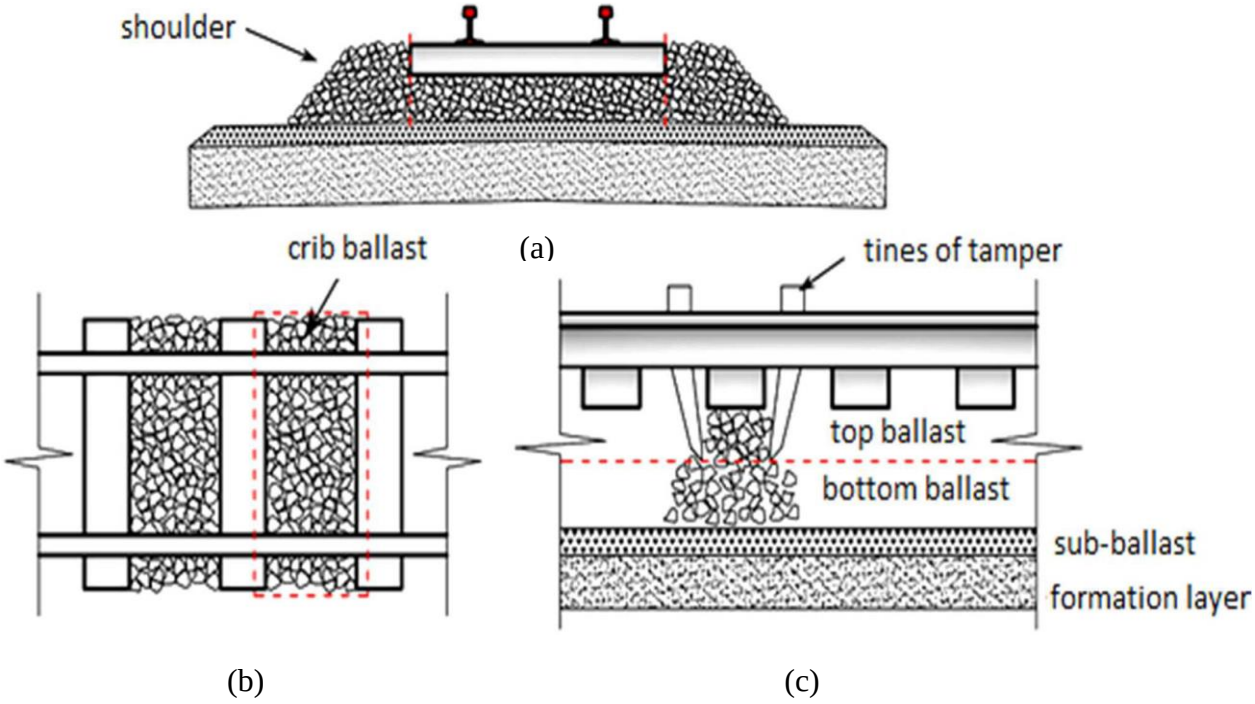


Figure 4: Schematic of Ballast Zones in Railway Track, (a) Cross-section, (b) Plan and, (c) Longitudinal Section

ii) **Shoulder ballast**. The shoulder ballast is located beyond the sleeper ends down to the bottom of the ballast layer. The main function of shoulder ballast is to protect the track from buckling.

iii) **Top ballast**. The top ballast is located below the sleepers and is disturbed by tamping.

Bottom ballast. It is located under the sleepers and is not disturbed by the maintenance process and is commonly the more fouled portion. The contribution of each part in playing the roles of ballast function to perform duties is presented in Table 1 [7].

Table 1: Contribution of ballast portions to perform ballast duties

Ballast Duties	Crip Ballast	Shoulder Ballast	Bottom Ballast	Top Ballast
Vertical Strength			✓	✓
Lateral Strength	✓	✓		✓
Longitudinal Strength	✓			✓
Resiliency			✓	✓
Adjusting and Track Levelling	✓		✓	✓

Ballast Duties	Crip Ballast	Shoulder Ballast	Bottom Ballast	Top Ballast
Drainage	✓	✓	✓	✓
Load Distribution and Dispersing			✓	✓
Prevent Growth of Plant	✓		✓	✓
Shock Absorption and Noise Attenuation	✓	✓	✓	✓
Electrical Resistivity	✓			✓
Subgrade Protection Layer	✓	✓	✓	✓

2.2. Ballast Assessment

The assessment of the physical, mechanical, and environmental properties of ballast is very essential in the selection of suitable quarry or predicting the remaining life of ballast. There are different specifications for evaluating the suitability of ballast for railway track which includes AREMA Specifications, European's Specifications, Australian's Specifications, and Canadian Specifications [7]. To perform well in track, the aggregate for ballast must have the following properties [12]:

a. Strength to resist the crushing action of superimposed track and dynamic traffic loading.

b. Hardness to resist abrasion at particle contacts and to withstand wear.

c. Toughness to resist breakdown by fracturing under impact loads.

d. Durability to resist abrasion and weathering.

e. Stability, to achieve this, the ballast needs to be a suitably graded and appropriate shape.

2.2.1 Load resistant characterization

Commonly available load resistance tests into an assemblage of grains are as follows [12]:

a. Impact test:

The relative measure of a ballast aggregate's resilience to rapid shock loads. A prepared sample of aggregates is layered in a steel mold in three roughly equal layers and each layer is given 25 tamping rod blows. The sample is subjected to 15 hits from a 14 kg hammer that falls freely from

a 380 mm height. The amount of fine material created after 15 blows is reported as a percentage of the sample's total mass. The smaller the percentage, the better the material; conversely, the higher the percentage, the worse the material.

b. Crushing value test:

The relative resistance of ballast aggregates to crushing when subjected to progressive loading. Three equal layers of aggregates are placed in a measuring cylinder and each layer is given 25 blows of the tamping rod. The material is transferred to the steel mmoldand leveled with a plunger in preparation for the crushing test. At the top of the specimen, a compression force is introduced and gradually increased to 400 kN within 10 minutes. The fine material created by the 400 kN application is reported as a percentage of the sample's total mass. The smaller the percentage, the higher the quality of the material; conversely, the higher the percentage, the poorer the quality of the material.

c. Los Angeles abrasion test:

The Los. Angeles. abrasion test is a widely used procedure for determining the toughness and abrasion characteristics of aggregates. Toughness is directly related to resistance to crushing and degradation, both of which are known to be major contributors to ballast settlement [15].

In this test, a sample of aggregates of either grade A-D or 1-3 and 12 steel balls of 5000g weight in total is placed on a large cylindrical drum and allowed to rotate at a speed of 30-33 rev/min for 1000 revolutions. The fine material generated after 1000 revolutions is expressed in a percentage of the total weight of the sample. The lower the percentage the better is the material and vice versa.

d. Deval abrasion test:

This test was developed in England for testing highway materials before being adopted by the railway sector. According to BR, this test is the most accurate predictor of ballast performance in service. It can be used to specify the minimal durability required to achieve the target ballast life with concrete sleepers in the British environment. A 5 kg specimen mass is rotated in a cylinder mounted on a shaft with the cylinder's axis inclined 30 degrees to the shaft's axis of rotation. The cylinder is rotated 10,000 times at a 30-33 revolutions per minute rate (rpm). Attrition is defined as the mass of particles created smaller than a 2.36 mm sieve, given as a percentage of the initial

specimen mass. This test can be performed with dry ballast particles or with an equal mass of clean water added to the dry specimen.

e. Mill abrasion test:

This is a wet abrasion test in which 3 kg of ballast and water are rotated for 10,000 revolutions at roughly 33 rpm in a 229 mm exterior diameter porcelain jar. This method of rolling wears out ballast without crushing it. The Mill abrasion value is the mass of material finer than a 0.075 mm sieve created by the test in comparison to the weight of the original sample. The mill abrasion test determines the aggregate mineral hardness, which was determined to be the most influential factor affecting the rate of buildup of permanent vertical deformation.

f. Clay lumps and friable particle test: Clay lumps and friable particles are defined in this test as those that can be broken with the fingers after the aggregate has been soaked in water for 24 ± 4 hours. Additionally, this test can be used in conjunction with the PSD test of ballast to assess the fines content, which may potentially fill in ballast voids.

2.2.2 Assessment of Stability Properties

Properties of ballast that relate to its ability to provide stable support are

(i) bulk density

The bulk density of the ballast is a significant factor in determining the track's performance in terms of vertical and lateral resistance to movement (holding capacity). As track mass grows, the track holding capacity improves as well. Additional material qualities that are connected to or have an effect on bulk density include the following:

a. Particle specific gravity: This is a critical factor in determining the bulk density of ballast (unit weight), which can be measured using the water displacement method. A higher specific gravity indicates that the track is made of a heavier material and has a greater degree of stability.

b. Absorption: Water absorption is a measure of a rock's porosity, which is proportional to its strength. The specific gravity test also includes an absorption component. Excessive absorption can result in rapid degradation during wetting and drying cycles, as well as freezing and thawing.

c. Rodded unit weight: The dry density of the ballast is determined in this test by compacting the ballast into a rigid cylindrical container with the aid of a steel rod. The container size is determined by the aggregate particle size and is typically 0.028 m3 in capacity with a height and diameter of 33 cm. Ballast

is deposited in three equal-height layers and each layer is vigorously tamped with steel rods twenty-five times.

(ii) Particle shape and texture

Raymond developed a form factor for railway ballast in collaboration with Canadian railroad research. Particles' shape and texture are theoretically determined by the ballast production process. A good interlock of ballast particles requires a minimum of elongated or flaky particles, for example, the rejection of slate-like rock sources. The study on the impact of shape properties on ballast discovered that a 20% increase in the percentage of flaky aggregates results in a 14.7 percent decrease in shear strength and a 5.2 percent decrease in friction angle, respectively, while a 25 percent aggregate limit by weight for misshapen particles is recommended to meet the Chinese standard's minimum shear stress level for flaky ballast [6]. While flaky and elongated particles result in a modest improvement in shear strength due to volumetric compaction in the absence of ballast breaking, unfavorable impacts of ballast fouling and degradation have been documented [16].

a. Flatness or flakiness: Flatness and flakiness are different names for the same shape characteristic. The British Standard (BS), BS EN933-3:1997 [12] defines a flaky particle as one in which the ratio of thickness to width is less than 0.6. The flakiness index is the percentage by weight of flaky particles passing the gauge shown in Figure 5.

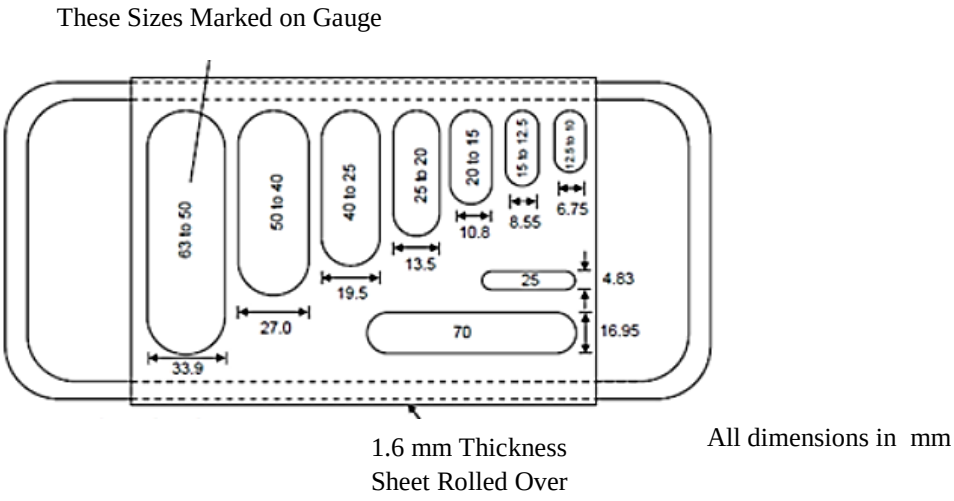


Figure 5: Flakiness index gauge

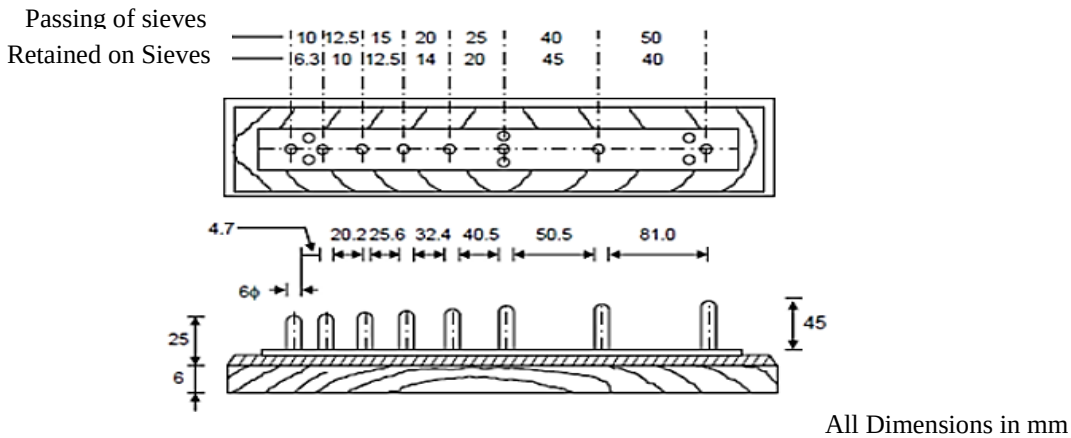


Figure 6: Elongation index gauge

b. Elongation: The British standard defines an elongated particle as one with a length-to-width ratio of more than 1.8. In both cases, the elongation index is the percentage by weight of elongated particles smaller than the slot on the gauge shown in Figure 6.

c. Sphericity: This test is a measure of how much the shape of a particle deviates from a sphere. The perfect sphere has a sphericity of one.

d. Angularity or roundness. This is a measure of the sharpness of the edges and corners of an individual particle.

e. Fracture particles: This test has been defined by the Canadian Pacific (CP) railroad. A fractured face is a freshly exposed rock surface with a minimum dimension of at least 1/3 the maximum particle dimension. A particle is considered fractured if it has 3 or more fractured faces.

f. Surface texture The surface texture has an important influence on ballast performance and it relates to the frictional characteristics of the fractured surface. However, there is no widely accepted test to measure this characteristic.

2.2.3 Assessment of weathering

The two tests commonly specified to assess the potential of aggregates to degrade or weaken due to weathering are:

a. Soundness test: This test simulates the weathering characteristics of an aggregate or more precisely its ability to resist the weathering process. The real test of soundness is where ballast particles are alternatively immersed and then dried using a salt solution. The salt solution that has been recommended by AREMA is Sodium Sulphate, although Magnesium Sulphate was suggested as a more appropriate

solution to use in this test. The importance of the soundness test will be more significant in regions where both atmospheric pollution and freeze-thaw are greatest.

b.Freeze-thaw breakdown.

This test is to check the resistance of ballast to frost action, swelling, and softening and uses oven-dry ballast particles which are immersed either partially or completely in water or a water-alcohol solution. The test indicates the ability of the ballast particles to retain water which could freeze and cause degradation during daily freeze-thaw cycles or could react chemically with minerals. This absorption test is carried out concerning the rainfall during the time of year freeze-thaw cycles occur and the impurities of the local rainwater where the material is to be used. Particles with fractured surfaces may offer more opportunity for penetration of water and hence for freeze-thaw degrading. Elongated, angular particles offer more surface area than smooth, spherical particles. Table 2 shows the recommended limit values for ballast material quality.

Table 2: Recommended limiting value for ballast materials quality (AREMA 200**7)** [12]

Ballast Material								
Property	Granite	Traprock	Quartzite	Limestone	Dolomitic	Blast	Steel	ASTM Test
% material passing No. 200 sieve **%**	1	1	1	1	1	1	1	C 117
Bulk specific gravity **a**	2.6	2.6	2.6	2.6	2.65	2.30	2.90	C 127
Absorption Percent	1	1	1	2	2	5	2	C 127
Clay lumps and friable particles **%**	0.5	0.5	0.5	0.5	0.5	0.5	0.5	C 142
Degradation %	35	25	30	30	30	40	30	b
Soundness (Soundness sulfate) 5 cycles **%**	5	5	5	5	5	5	5	C 88
Flat and/or elongation particles **%**	5	5	5	5	5	5	5	D 4791

a Limits for the whole test shows the maximum value except for the bulk specific gravity value

b Gradations containing particles retained on a 25 mm sieve shall be tested by ASTM C 535.

Gradation with 100% passing on a 25 mm sieve shall be tested by ASTM C 131. Use grading most representative of ballast material.

2.2.4 Cementing characteristics of ballast

Cemented ballast refers to a variety of circumstances ranging from damp to dry, extensively fouled ballast to ballast conditions in which coarse particles are linked together in a matrix structure. Chemical processes, capillarity attraction (as a result of fouling materials), or a secondary bonding mechanism can all be used to create bonding in ballast. By soaking the ballast in water, one may determine the sort of cementing that has occurred. Chemical bonds will remain strong in the water, whereas other forms of bonds would deteriorate and disintegrate.

2.2.5 Identification of ballast composition

According to Boucher and Selig, the performance of ballast in the track is determined by factors other than field conditions, particle shape, and grading [12]. The petrographic analysis uses a hand lens or a low-powered microscope to study samples of freshly broken rock to ascertain the mineralogical features that will aid in the selection of an appropriate quarry. The value of petrographic analysis is highly dependent on the petrographer's ability to match facts provided about the material's source and intended use with the findings of the petrographic investigation. Chemical analysis is also required to support petrographic analysis because it determines the type and percentage of constituent elements in a material as well as identifies and estimates the potential for chemical breakdown. This analysis, which often uses standard analytical chemistry techniques and X-ray diffraction, is mainly beneficial for fines in ballast, while petrographic analysis of visible rock particles is usually sufficient. Table 3 and Table 4 contain information about the ballast qualities and requirements [7]**.**

Table 3: Track ballast layer specification indices

Ballast properties	**Characteristics**	**Test method**	**Terms of evaluation**
Mechanical	Hardness &Toughness	Los Angeles	Abrasion, Attrition, and fragmentation
	Hardness	Deval attrition test (dry, wet)	Surface abrasion test
	Hardness	Micro Deval	Surface abrasion test
	Toughness	Aggregate Crushing Value	Fragmentation and crushing resistance
	Hardness	Scratch(Mohs)Hardness	Surface abrasion to produce fines
	Toughness	Point load Strength	Fragmentation(splitting)
	Toughness	Aggregate impact Value	Aggregate resistance to sudden shock, fracturing

Ballast properties	Characteristics	Test method	Terms of evaluation
Mechanical	Hardness	Dorry abrasion	Surface abrasion to produce fines
	Hardness	Mill abrasion	Surface abrasion to produce fines
	The clue to Hardness, toughness and soundness	Petrography analysis (intact particles/Fines)	Mineralogy, Chemical alteration
Physical	Gradation	Particle size distribution ability	Compaction energy and drainage ability
	Gradation	Fineness of material	Drainage
	Stability	Particle density	Stability and indirect toughness
	Stability	Bulk density	Interparticle void, drainage, and track stability
	Shape index	Particle shape	Fragmentation(splitting) and drainage
Environmental	Soundness	Dry-wet	Durability and weathering resistance
	Soundness	Freeze and Thaw	Durability and weathering resistance
	Soundness	Water absorption	Saturation and weathering resistance
	Soundness	Aggregate Porosity	Durability and weathering resistance
	Soundness	Magnesium/Sodium sulfate resistance	Durability and weathering resistance
	Soundness	Friable particles, clay lumps	Durability and preliminary abrasion
Geometrical	Cross Profile	Thickness	Track structural stability, resiliency, and damping
		Shoulder width	Track lateral stability
		Side slope	Track structural stability
	Layer Deviation	Unevenness, misalignment	Track stability to ride comfortably

Table 4: Track ballast assessment based on the proposed categorization of ballast technical requirement

Test zone	Requirements		Australia (AS 2758.7) (2009)	Europe EN13450 (2003)	USA AREMA(2012)
Physical	Particle size distribution (PSD)		AS 1141.11.1	EN933-1	ASTM-C136
	% material passing No. 200 sieve %		Max 1 % AS 2758.7	Max 0.5-1.5 % (0.063mm) EN 933-1	Max 1% ASTM-C117
	Clay lumps and friable particles %		--	--	Max 0.5 % ASTM-C142
	Particle Density (Specific gravity)		Min 2.5 t/m3 (dry)	EN1097-2 CEN ISO/TS17892-3	Min 2.6 t/m3 ASTM-C127
	Bulk Density (unit weight)		Min 1.2 t/m3 (AS1141.4) NSW Min 1.4 t/m3	CEN ISO/TS 17892-2	Min 1.12 t/m3 C29
	Misshapen particles	Elongation	2:1 ratio Max 30% 3:1 possible Alt.	3:1, Max 4-12% EN 933-3 Length>100mm <6%	Max 5 % ASTM D4791 3:1
		Flakiness	Max 30 % AS1141.14	Max 15-35 % EN 933-3 (1997)	Max 5 % ASTM D4791
		Crushed Surface (texture)	Min 75 % by mass, 2 crushed faces	--	--
Environmental Soundness and resistance to the weathering	Water absorption%		--	EN1097-6	Max 1 - 2% ASTM-C127
	Freeze and Thaw Cycle		--	EN-NS 1367-1 (20 cycles)	--
	Sulfate test		--	EN 1367-2 (1% NaCl-10 cycle)	Max 5 % ASTM-C88 (5 cycles)
	Clay lumps and friable particles %		--	--	Max 0.5 % ASTM-C142
Mechanical		Micro-Deval	--	Max 5 – 15% EN 1097-1	--

Test zone	Requirements		Australia (AS 2758.7) (2009)	Europe EN13450 (2003)	USA AREMA(2012)
Mechanical	Wet Attrition test	Mill Attrition Test	--	----	AN= LAA+5MA* 25%<AN<65%
		Wet Attrition Value (WAV)	Max 6%,8%,12 % based on class of track 1141.27	---	----
	Toughness Fragmentation And fracturing resistance	Los Angles Value (LA)	Max 25 %, 30%, 40% based on class of track (1141.23)	Max 12 to 24 % EN 1097-2	Max 30% ASTM-C535-C131
		Aggregate Crushing Value (ACV)	Max 25%, 30%, 40% based on class of track (AS 1141.21)	---	--
		Impact Value (IV)	---	14%<IV<22% EN1097-2	
		Strength	Wet : Min 175 KN , 150 KN , 110 KN Wet/dry variation: max 25%, 30%,40% Based on track class AS 1141.22	--	Point load test Dry>1200 kg Wet>800
		Drainage	--	CEN ISO/TS 17892-11	--
		Electric Conductivity	Min 60 Ohm.m 1289.4.4.1	--	--
Mainline	Ballast Depth the underside of the sleeper to the top of the finished formation		325, 275, 225 mm based on the class of track	--	>12 in** Main line

Test zone	Requirements	Australia (AS 2758.7) (2009)	Europe EN13450 (2003)	USA AREMA(2012)
Ballast profile (Geometry of layer)	Ballast shoulder width	400-700 mm (CWR, LWR***) 300-700 mm Loose rail	--	>12 in (CWR) Main line
	Side Slope of the bMainlineoulder	Height: horizontal 1:1.5	--	Height: horizontal 1:2
	Crib zone	To the top level of sleeper	--	--

*Abrasion Number is an index that included Los Angeles and mill abrasion loss.

**The measurement is made under the line rail in tangent track, or under inside rail in curved track, and is made with respect to the top of the sub-ballast at the centerline.

***CWR: continued welded rail, LWR: long welded rail

2.3. Gradation(Particle Size Distribution)

The grain size distribution (gradation) of ballast is used to specify new ballast and is a frequently used technique for determining the volume of in-service ballast [17]. Gradation of ballast is critical for track strength, deformation, deterioration, stability, and drainage[3]. Ballast that has been graded properly results in denser packing, improved frictional interlock, and thus less settlement. Broader ballast gradations are preferable to narrow gradations in terms of strength. However, in addition to durability, fines storage volume, and size segregation must be considered.

All ballast requirements, on the other hand, require uniform gradation to ensure proper drainage. Ballast that is uniformly graded settles faster and is also more prone to breaking than ballast that is well graded [3]. Typically, standards for mainline ballast specify a rather restricted range of particle sizes to maximize interparticle void volume [17]. This enormous void volume allows for drainage and storage of ballast fouling particles. The specifications for ballast grading demand a uniform grading with a uniformity coefficient of 1.5 to 3 [18]. To minimize ballast deformation and degradation, Indraratna et al. (2006) recommended using slightly graded ballast (Cu =2.3-2.6) rather than the more common uniform grading with Cu of about 1.5. When compacted sufficiently, narrowly graded ballast performs admirably and provides excellent drainage and fouling material storage. Although more broadly graded ballast provides increased strength and resistance to deformation due to the particles' denser packing arrangement, it is

expected to have a lower void volume than narrowly graded ballast. While a more extensively graded ballast may provide increased deformation resistance and adequate drainage and fouling material storage capacity, the ultimate issue becomes material handling and transport, as the particles will tend to segregate during transport to the site [17].

The gradation of the ballast as it is placed is important to its function and is frequently the most difficult to determine. Keeping in mind the American Society of Testing Materials (ASTM) sample size standards, it is also critical to adhere to sampling guidelines when analyzing field placement [17].

2.3.1.American ballast specification

Various materials were used for railway ballast in the early years of the railroad business in the United States to support the track superstructure. Almost any ballast material that could be obtained cheaply was employed and found to be suitable when subjected to traffic loading [12]. Granite, trap rocks, quartzite, dolomites, and hard limestone were all commonly regarded as acceptable for ballast in the United States. Since limestone dissolves into fine particles that cement together, it is not the best ballast material if alternative hard rock material is economically available. AREMA has suggested the following ballast gradings in Table 5. The gradation for railway ballast that is most frequently used is depicted in Figure 7.

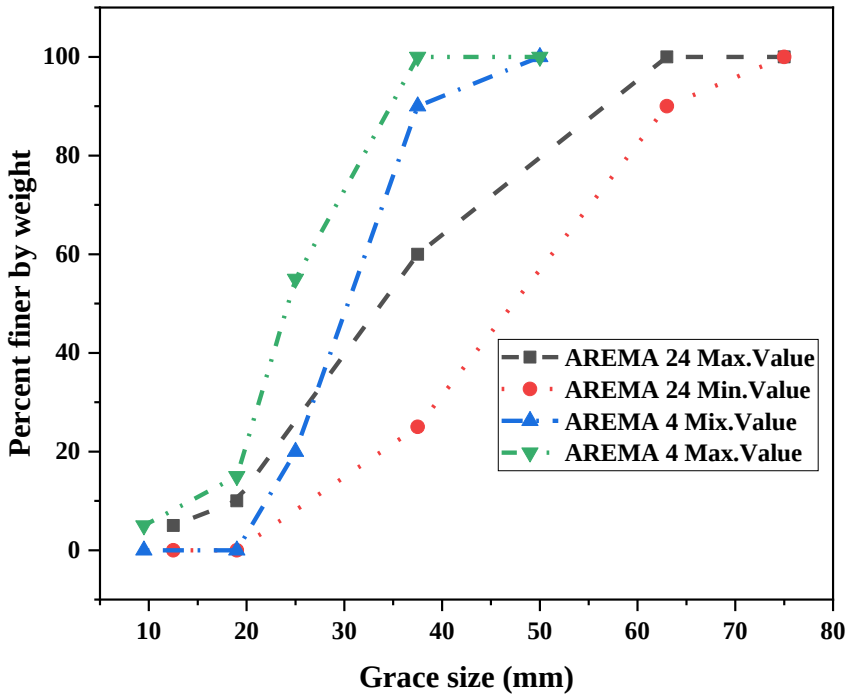


Figure 7: AREMA #24 and #4 ballast gradation particle size ranges

Table 5: Recommended AREMA ballast gradings (after AREMA, 2000)

AREMA No	Nominal size (mm)	Percentage passing (%)									
		75 mm	63 mm	50 mm	37.5 mm	25 mm	19 mm	12.5 mm	9.5 mm	4.75 mm	2.36 mm
24	63–19	100	100-90		60-25		10-0	5-0	-	-	-
25	63–9.5	100	100-80	85-60	70-50	50-25	-	20-5	10-0	3-0	-
3	50-25	-	100	100-95	70-35	15-0	-	5-0	-	-	-
4A	50-19	-	100	100-90	90-60	35-10	10-0	-	3-0	-	-
4	37.5-19	-	-	100	100-90	55-20	15-0	-	5-0	-	-
5	25-9.5	-	-	-	100	100-90	75-40	35-15	15-0	5-0	-
57	25-4.75	-	-	-	100	100-90	-	60-25	-	10-0	5-0
Note 1: Grading number 24, 25, 3, 4A, and 4 are main line ballast materials. Grading number 5 and 57 are yard ballast materials.											

Table 6: Modified AREMA No.3 grading (after Norfolk Southern Corporation, 2011)

Sieve Size (mm)	**Percentage passing (%)**	
	AREMA 3	**Modified 3**
63.0	100	100
50.0	100-95	100-95
37.5	70-35	65-30
25.0	15-0	15-0
12.5	5-0	5-0

The AREMA No. 4 classification corresponds to the American Standard Testing for Material (ASTM) C33 classification. Furthermore, ASTM C33 grade 56 is quite close to AREMA grade 5. The majority of railroads in the United States employ AREMA gradings; Norfolk Southern Corporation (NSC) modified AREMA grading No. 3 for heavy tonnage lines and uses AREMA grading No. 5 for the yard [12]. Table 6 summarizes the modifications made by NSC to the AREMA No 3 grading. Figure 8 demonstrates that NSC has increased the amount of larger ballast particles.

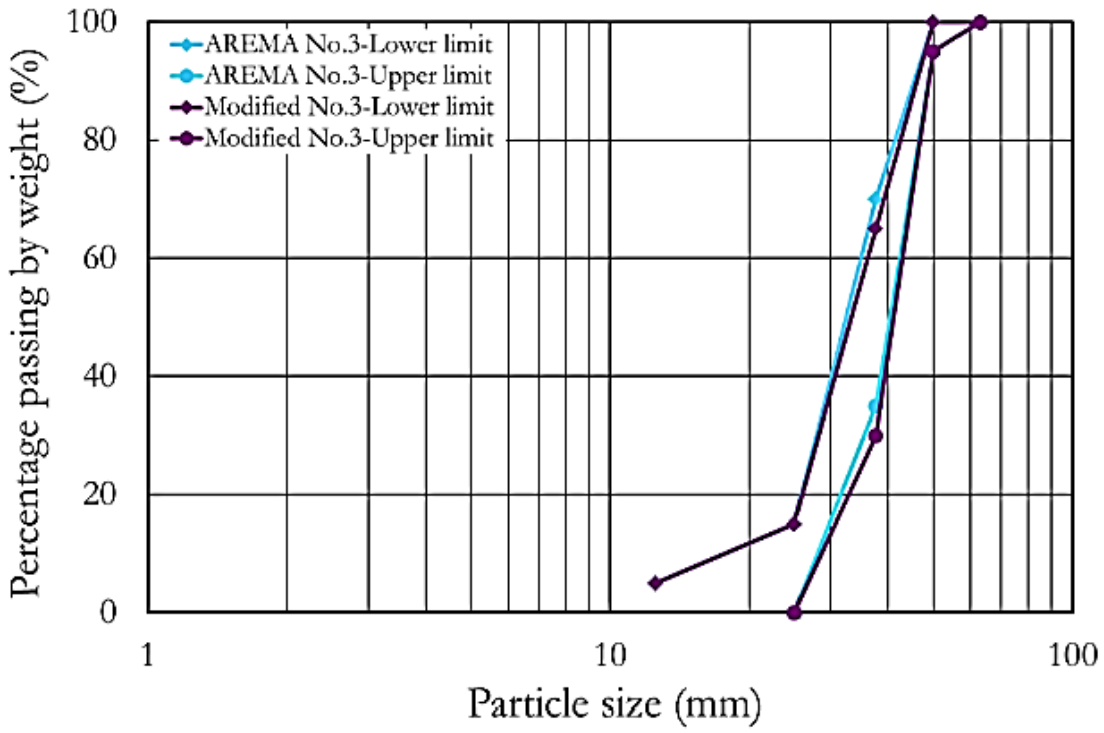


Figure 8: PSD of modified AREMA No 3 used by NSC

2.4. Ballast Degradation Mechanisms.

Ballast degradation has a major contribution to uneconomical maintenance costs and shortening of the service life of the railway system. Generally, the main indicator of ballast degradation is ballast fouling.

2.4.1.Ballast fouling

Ballast fouling is the contamination of ballast with fines caused by particle breaking caused by repeated traffic loads, sleeper wear, fines infiltration from underlayers, coal fines, and surface spills. Ballast fouling is mostly caused by ballast fracture, which accounts for around 76% of fines [11]. When first put, the ballast layer has approximately 45% vacant space [19], with asperities of one particle resting on the surfaces of other particles to form a stable ballast matrix with a high shear resistance. The point of contact between asperities and particle surfaces is referred to as the interparticle contact point, and it is utilized to transfer load from one particle to another and ultimately to the underlayers (sub-ballast and subgrade). The majority of energy is absorbed within the ballast structure during the load transfer mechanism, while the remainder is transferred, which is why ballast aggregates must be strong. Asperities will break and fill the spaces between the particles due to the passage of traffic, forming a durable ballast layer. The ideal resilience in a ballast layer is elastic, which means that deformation is reversible and the ballast returns to

its pre-loading position [11]. Due to the large loads involved and the narrow contact area, each ballast particle deforms significantly, potentially resulting in particle breakage or contact wear when the applied stress approaches or surpasses the strength. Ballast resilience is achieved through the interparticle contact sites between the ballast particles, which allow for significant vertical and lateral elastic deformation as long as the ballast stress is tolerable and the ballast does not degrade. The passage of traffic compacts and consolidates the ballast layer, resulting in a transient increase in the layer's strength and stability as a result of densification. As loading cycles and magnitudes increase, abrasion and crushing of the particles occur, resulting in progressive plastic deformation and reduction of interparticle voids with time and usage. When the void space in the ballast layer becomes clogged with fouling material, the necessary free movement of nearby particles is restricted, preventing the compaction and consolidation process from occurring. As ballast fouls, it partially fills the vacuum area, resulting in decreased drainage capacity. However, decreased drainage capacity and repeated loading of heavily fouled ballast frequently result in the ballast particles being forced apart by the fouling material, either mechanically or because the fouling material reduces friction at interparticle contact points, thereby releasing some of the interparticle compressive force and reducing the ballast's and track structure's stability. The most obvious sign of fouling material is frequently a muddy slurry. When loaded with big particles in dry conditions, fouled-ballast tends to shift the weight to the weak fines, resulting in random dispersion of the large particles. When particles reach saturation, mud and slurry are formed.



(a) Clean ballast (b) Partially fouled ballast (c) Heavily fouled ballast

Figure 9: Critical ballast fouling phases [12]

Additionally, in the absence of an adequate sub-ballast layer or the presence of sub-ballast that is poorly graded, clay and silt size particles frequently build in the ballast layers. Under cyclic train stress, these fine-grained soils are generated from saturated subgrade soil (jetting action) and travel through the void spaces of sub-ballast and ballast layers, speeding the fouling process. Fouling material impairs the track's

drainage capability, resulting in the development of internal pore water pressures during wet circumstances.

Additionally, the crushed ballast particles and fine particles that migrate as a result of clay pumping form a thin layer around the bigger aggregates, reducing friction and boosting ballast compressibility and lateral flow. Given the harmful effect that fines have on railway track performance, it is critical to establish appropriate criteria for estimating the extent of ballast layer fouling. Both under- and over-estimation of ballast fouling degree results in excessive maintenance expenses. Underestimating the degree of fouling may result in rapid deformation and track failure in general. By contrast, overestimating the degree of fouling may result in shorter ballast-cleaning cycles, hence shortening the ballast's life [19].

2.5. Quantification of Ballast Particle Breakage

Progressive breaking of the ballast particles occurs as a result of repeated axle loads. Particle breakage has been shown to have a considerable effect on the strength and deformation behaviors of granular soils, such as railroad ballast and sand [16]. The amount of particle crushing that occurs in a soil element (ballast particles) when loaded is dependent on the following factors: (a) particle size distribution; (b) particle shape; (c) effective stress state; (d) effective stress path; (e) void ratio; (f) particle hardness (hardness of cementing material or weakest constituent of a particle and weakest particles of an element); and (g) the presence or absence of water [20]. The degree of particle breakage is defined by the particle size distribution curves of soil samples (ballast particles) collected before and after loading [20]. Researchers have devised the following methods for determining particle breakage:

(i) Relative Breakage (Br) [20]
(ii) Ballast Breakage Index(BBI) [21].
(iii) Marsal's breakage (Bg) [22]
(iv) Breakage ratio (B) [23]
(v) Fouling index (FI) [1]

Relative Breakage (Br) is a breakage index calculated by dividing the breakage potential Bp by the total breakage [20]. The area between the line defining the upper limit of silt size, D = 0.074 mm, and the portion of the particle size distribution curve with D > 0.074 mm is the breakage potential of particles, where the unit area is the area of one log cycle as shown in Figure 10. The total breakage equals the area between the PDS curves before and after loading, as defined by the upper silt size limit, D=0.074, as shown in Figure 11.

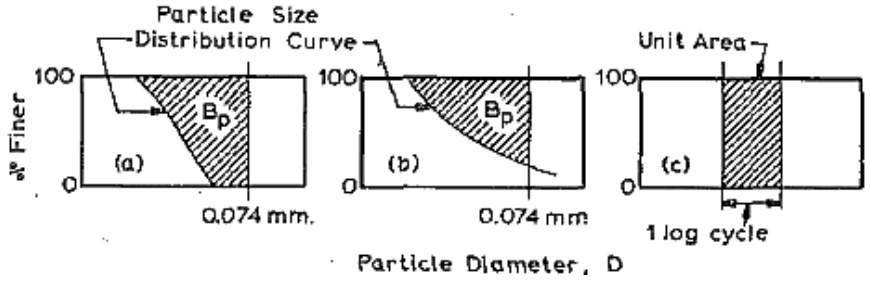


Figure 10: Definition of Breakage Potential (Bp) [20].

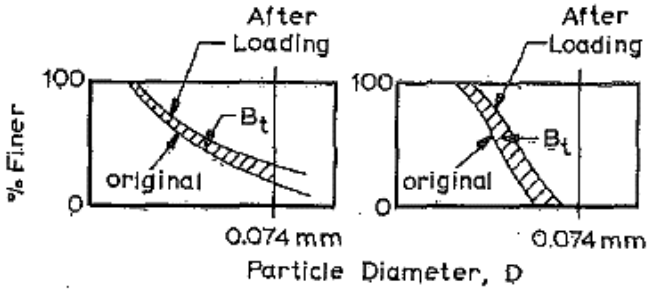


Figure 11: Definition of Total Breakage (Bt) [20].

Ballast Breakage Index(BBI) is an index introduced by Indraratna et al, for quantifying the degree of railway ballast degradation [21]. This index is given as the ratio of the area between the initial and final PSD curves and the area between the initial PSD curve and arbitrary boundary of maximum breakage as shown in Figure 12 [23]. It is noted that the BBI has a lower limit of 0 (no breakage) and an upper limit of 1.

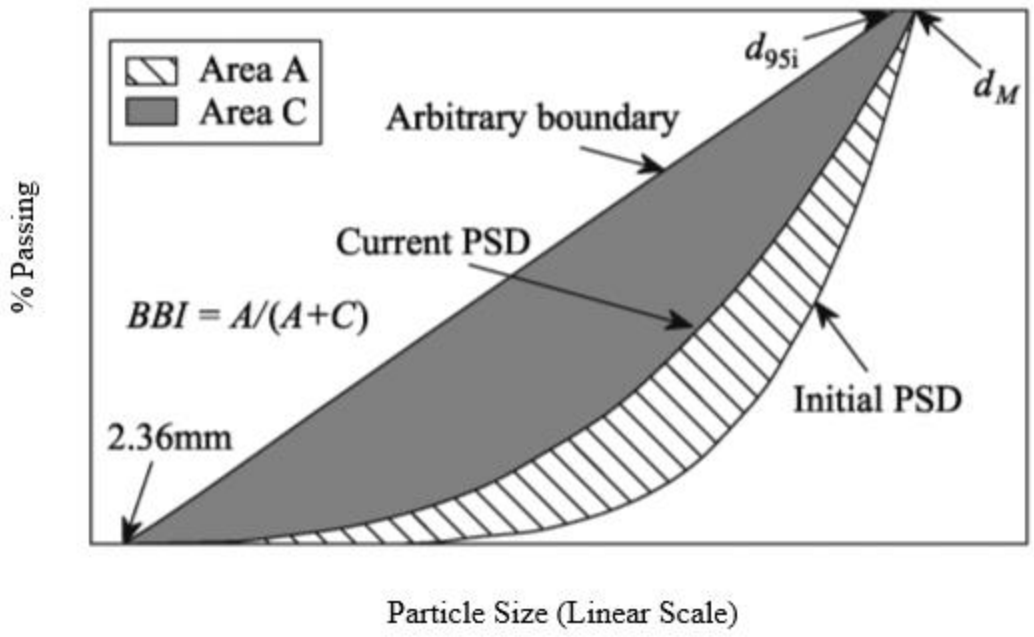


Figure 12: Definition of Ballast Breakage Index (BBI) [16].

Breakage ratio (B) refers to the ratio of the area between initial and final PSD curves to the area between fractal and Initial curves, whereby all PSD curve is limited by the Ultimate PSD line at diameter, D=0.074mm as shown in Figure 13.[23]. The fractal PSD is defined as

$$F(d) = \frac{d^n - d_m^n}{d_M^n - d_m^n} \times 100\% \qquad 2.1$$

n = Fractal dimension, d_m = Smallest possible particle, d_M =Maximum particle size.The value of n is assumed around 0.4 for most practical purposes [1]

Fouling Index (FI) is defined as the total fraction of dry weight passing through the 4.75 mm (No. 4) sieve as well as 0.075 mm (No. 200) sieve [1]. The FI is computed by the following equation:

$$FI = P_4 + P_{200} \qquad 2.2$$

P_4 = Percentage of material passing through the 4.75mm (No.4) sieve

P_{200} = Percentage of material passing through the 0.075mm (No. 200) sieve

The classifications of ballast fouling index done according to Table 7.

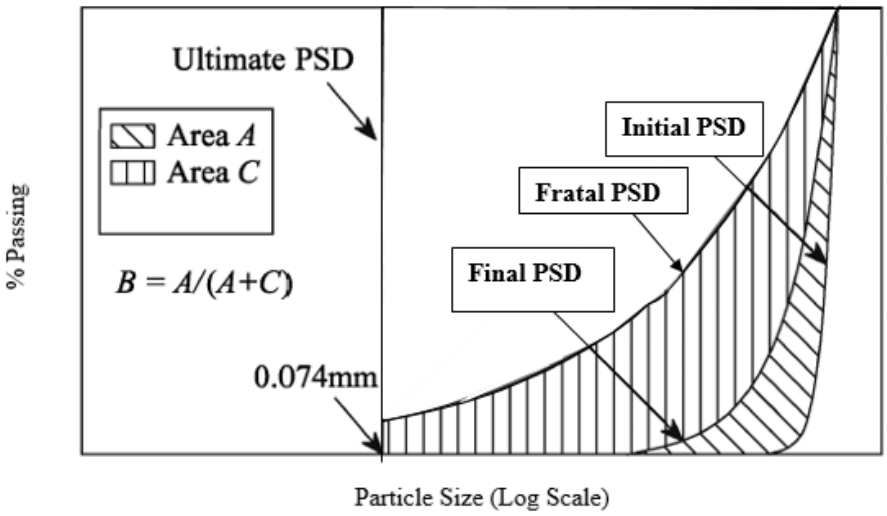


Figure 13: Definition of Breakage Index, B.

Table 7: State of ballast degradation based on FI according to Selig and Waters,1994 [24]

Range of Calculated Fouling Indices	Ballast Degradation State
< 1	Clean
1 to < 10	Moderately Clean
10 to < 20	Moderately Fouled
20 to < 40	Fouled
≥ 40	Highly Fouled

Marsal's breakage (Bg) is a percentage increase in the amount that passes through each sieve size [23]. This method entails altering the aggregates' overall grain size distribution following the application of a load and then performing sieve analysis on specimens before and after each test. The difference in percentage retained on each sieve size is calculated from the changes in particle gradation (Wk = Wki – Wkf), where Wki represents the percentage retained on sieve size k before the test and Wkf represents the percentage retained on the same sieve size after the test. There are some positive and some negative differences; indeed, the sum of all positive values of Wk must theoretically equal the sum of all negative values. The breakage index Bg is the sum of the positive values of Wk expressed as a percentage, with a theoretical lower limit of zero indicating no particle breakage and a theoretical upper limit of unity (100 percent) indicating that all particles have been broken to sizes smaller than the smallest sieve size used. Marsal Breakage Index was used in this study due to its ease of computation and ability to provide a numerical value indicating the degree of particle degradation [3].

2.6. Permeability of Ballast

Flow through porous media such as ballast and sub-ballast is usually determined using Darcy's law:

$v = ki$

Where, v = average velocity of the fluid, i = hydraulic gradient, and k is the coefficient of permeability (hydraulic conductivity). The best way to evaluate the value of k for a particular porous medium is by conducting field or laboratory experiments such as constant head or falling head permeability tests. However, many researchers have presented several empirical formulae based on the characteristic grain size of the medium to model permeability. Hazen's formula can be used to estimate the permeability of granular aggregates[3] [25]:

$$k = C(D_{10})^2 \quad 2.3$$

Where k is the coefficient of permeability and C is an empirical constant that varies in the range of 40–150. This relationship was developed by Hazen based on tests with filter sands used for water purification, for which the D_{10} sizes were between 0.1 and 3 mm and the coefficient of uniformity was less than five [25]. The advantage of Hazen's formula is that D_{10} from a large number of samples at a given site can be quickly and easily determined to compute permeability. This helps evaluate the variability of permeability at a given site quickly and cost-effectively.

Indraratna and Vafai suggested that the permeability of granular materials can be better represented by the following empirical formula [3].

$$k = \alpha(D_5 \times D_{10})^{\beta} \quad 2.4$$

Where α and β are two empirical constants.

Alyamani and Sen proposed the following equation which is more applicable to well-graded soils [26].

$$k = 1.5046[I_0 + 0.025(D_{50} - D_{10})]^2 \quad 2.5$$

Where k = permeability (m/day), and I_o is the x-intercept of the slope of the line formed by D_{50} and D_{10} of the grain-size distribution curve (mm).

The Alyaman and Sen formula is very sensitive to gradation change and it depends only on particle size distribution. In this study, Alyaman and Sen empirical for permeability were used to assess the effect of ballast degradation on the permeability of the ballast layer.

3. MATERIALS AND METHODOLOGY

3.1. Literature review

Moaveni et al. [27], investigated the morphological characteristics of railroad ballast degradation trends in the field and laboratory to gain a better understanding of the effect of heavy axle load traffic on ballast degradation. The Los Angeles abrasion test was used to determine the abrasion of the ballast, as well as the installation of ballast steel boxes in both the curve and tangent zones, where surface and form changes were captured using an Image Analyzer. The study's findings indicate that the magnitudes and rates of deterioration and breakage, as well as changes in the morphological features of particles, were quite different between the LA abrasion test and field degradation caused by frequent traffic loading. The author concluded that a complete investigation employing improved ballast sample and testing methodologies is necessary to elucidate the mechanisms of ballast degradation.

Bian et al. [28], conducted Abrasion Testing, and Computer-Aided Morphology Analysis to quantify railway ballast degradation to determine the effect of ballast abrasion on the performance of ballast material. The author discovered that LA abrasion testing provides useful information on the ballast bed degradation caused by train traffic loads and maintenance tamping.

Guo et al. [29], performed Los Angeles Abrasion Test and Image Analysis to determine and evaluate how individual particle morphology (size and shape) changes during ballast degradation, and to verify the assumptions that ballast degradation is primarily caused by sharp corner loss and that flaky or elongated particles are more prone to break. The test results indicate that ballast degradation is directly related to the morphology of the ballast particles as follows: (a) LAA loss is greater for flaky or elongated particles than for cubic particles, implying that flaky or elongated ballast particles will deteriorate more severely; (b) flaky or elongated particles are more prone to cracking than cubic particles, and (c) larger ballast particles crack more easily. The author stated that the method, which combines LAA testing with 3-D image analysis, enables quantification of ballast deterioration, particularly in cases of abrasion degradation of individual ballast particles.

Jing et al. [6]. conducted a series of large-scale direct shear tests to determine the breakage and fines content of ballast samples classified by flakiness and elongation index. The results indicated that aggregates' strength and friction angle decreased by 14.7 percent and 5.2 percent, respectively, while their flaky aggregate proportion increased by 20%. While flaky and elongated aggregates have a higher shear

strength at low vertical stresses than cubic aggregates, they degrade faster and have a shorter service life over time.

3.2. Field Investigation

This investigation involves visual inspection of the condition of ballast like the growth of weeds and fine concentration on the track ballast. As the amount and composition of ballast fines are difficult to quantify visually, the severity ranking criteria relies strongly on the presence of vegetation growth within the ballast. At the lowest severity level, vegetation growth is present within the ballast but does not interfere with the visual ballast inspection, while at the highest severity level, the vegetation is deemed dense enough to interfere with train movements. This visual ballast assessment methodology, while straightforward to implement, cannot detect the accumulation of fines within the ballast without any surface expression and, in absence of any vegetation growth, the severity of the ballast degradation cannot be easily differentiated.

3.3. Samples and sampling procedures

3.3.1.Sampling according to AASHTO R 90

The sampling was done at railway track sections from different locations whereby three points were selected randomly in each location . Full-depth increments of approximately equal size from each location on the three points were obtained. The increments from the three points were combined to form a single sample for the specified location.

3.3.2.Reducing Samples to Test Size according to ASTM C702 [30]

The field samples were reduced to an appropriate size for testing the required characteristics of ballast following ASTM C702 by Method B (quartering). The method involves thoroughly mixing, cone formation, cone flatten followed by dividing the flattened cone into four equal portions. The opposite quarters were retained and the rest two were rejected.

3.4. Material Testing

3.4.1.Gradation (Sieve Analysis)According to ASTM C117 and C136 [31]and [32].

The sample sizes were chosen depending on the Nominal Maximum Size of Aggregate as shown in Table 8. In this study, 35kg were chosen as a test sample and dried in an oven at 110 $\pm 5°$ C for 24 hours then cooled to room temperature. The material finer than 0.075mm was removed according to ASTM C117 and the material larger than 0.075mm was measured according to ASTM C136 by selecting sieve sizes according to specification requirements. The material retained in each sieve was recorded and expressed in percentage. The percentage of material passing in each sieve was calculated and recorded.

Table 8: Test sample sizes for aggregate gradation test

Sizes for Aggregate Gradation Test Nominal Maximum Size*		**Minimum Dry Mass**	
mm	**(in.)**	**(g)**	**(lb)**
125	(5)	300,000	(660)
100	(4)	150,000	(330)
90	(3 1/2)	100,000	(220)
75	(3)	60,000	(130)
63	(2 1/2)	35,000	(77)
50	(2)	20,000	(44)
37.5	(1 1/2)	15,000	(33)
25.0	(1)	10,000	(22)
19.0	(3/4)	5000	(11)
12.5	(1/2)	2000	(4)
9.5	(3/8)	1000	(2)
6.3	(1/4)	1000	(2)
4.75	(No. 4)	500	(1)

3.4.2. Los Angeles Abrasion according to ASTM C535 [33]

The resistance of the ballast material to abrasion and wear was assessed according to ASTM C535. The test sample size was chosen according to the grading of the test sample as shown in Table 9 and the number of balls was chosen according to grade number as shown in Table 10. For this project, 10kg sample and

12 steel balls of 500g each were placed in an abrasion machine drum rotating with 30-33rpm to provide 1000 revolutions. The materials are removed from the drum after the specified revolution and sieved on Sieve #12 (1.7mm standard sieve size). The Los Angeles Abrasion Value is calculated as the percentage of material passing Sieve #12 as given in equation 3.2.

$$\text{Los Angeles Abrasion Value} = \frac{(\text{Original Weight} - \text{Weight Retained on \#12}) \times 100}{\text{Original Weight}} \qquad 3.2$$

Table 9: Gradings of Test Samples

Sieve Sizes		Mass of Indicated Sizes (g)						
Passing	Retained	A	B	C	D	1	2	3
76.2 mm (3 in)	63.5 mm (2.5 in)	—	—	—	—	2500 ± 50	—	—
63.5 mm (2.5 in)	50.8 mm (2 in)	—	—	—	—	2500 ± 50	—	—
50.8 mm (2 in)	37.5 mm (1.5 in)	—	—	—	—	5000 ± 50	5000 ± 50	—
37.5 mm (1.5 in)	25.0 mm (1.0 in)	1250 ± 25	—	—	—	—	5000 ± 25	5000 ± 25
25.0 mm (1.0 in)	19.0 mm (3/4 in)	1250 ± 25	—	—	—	—	—	5000 ± 25
19.0 mm (3/4 in)	12.5 mm (1/2 in)	1250 ± 10	2500 ± 10	—	—	—	—	—
12.5 mm (1/2 in)	9.5 mm (3/8 in)	1250 ± 10	2500 ± 10	—	—	—	—	—
9.5 mm (3/8 in)	6.3 mm (1/4 in)	—	—	2500 ± 10	—	—	—	—
6.3 mm (1/4 in)	4.75 mm (#4)	—	—	2500 ± 10	—	—	—	—
4.75 mm (#4)	2.36 mm (#8)	—	—	—	5000 ± 10	—	—	—
TOTAL		5000 ± 25	5000 ± 20	5000 ± 20	5000 ± 10	10000 ± 100	10000 ± 75	10000 ± 50

Table 10: Number of abrasive charges for above samples

Abrasive Charges	No. of Revolutions	No. of Spheres	Weight of Charges
			(g)
A	500	12	5000 ± 25
B	500	11	4584 ± 25
C	500	8	3320 ± 20
D	500	6	2500 ± 25
1	1000	12	5000 ± 25
2	1000	12	5000 ± 25
3	1000	12	5000 ± 5

3.4.3.Flakiness Index According to BS812:1989 [34].

The misshape of ballast aggregate was assessed according to BS812:1989 for Flaky particles. The size of the test sample was chosen according to Table 11. The flakiness index of an aggregate sample is found by separating the flaky particles and expressing their mass as a percentage of the mass of the sample tested in Table 12. The test does not apply to material passing a 6.30 mm BS test sieve or retained on a 63.0 mm BS test sieve. The portions of mass passing and retained in sieves are shown in Table 12 were recorded as M1 and gauged with flakiness gauge. The mass of material passing the slots of the flakiness gauge are recorded as M2. The Flakiness Index of each portion was calculated as given in equation 3.3.

$$\text{Flakiness Index (FI)} = \left(\frac{M_2}{M_1}\right) \times 100 \qquad 3.3$$

The Flakiness Index of the sample equals the summation of Flackiness Indices of individual portions.

Table 11: Minimum mass of test portion

Nominal Size of Material (mm)	Minimum Mass of Test Portion After Rejection of Oversize and undersize particles (kg)
50	35
40	15
28	5
20	2
14	1
10	0.5

Table 12: Data for Determination of Flakiness Index

Aggregate Size Fraction		Width of Slot in thickness gauge or special sieves (mm)	Minimum mass for subdivision (kg)
BS Test Sieve Size			
100% Passing	100% Retained		
50.0	37.5	26.3±0.3	35
37.5	28.0	19.7±0.3	15
28.0	20.0	14.4±0.15	5
20.0	14.0	10.2±0.15	2
14.0	10.0	7.2±0.1	1
10.0	6.30	4.9±0.1	0.5

3.4.4.Elongation Index According to BS812:1990 [34].

The misshape of ballast aggregate was assessed according to BS812:1990 for elongated particles. The size of the test sample was chosen according to Table 13.

Table 13: Data for Determination of Elongation Index

Aggregate Size Fraction		Gauge	Minimum Mass for Subdivision (kg)
Test Sieves (mm)			
100% Passing	100% Retained		
50.0	37.5	78.7±0.3	35
37.5	28.0	59.0±0.3	15
28.0	20.0	43.2±0.3	5
20.0	14.0	30.6±0.3	2
14.0	10.0	21.6±0.2	1
10.0	6.3	14.7±0.2	0.5

The elongation index is found by separating the elongated particles and expressing their mass as a percentage of the mass of the sample tested. This test does not apply to material passing a 6.30 mm test

sieve or retained on a 50.0 mm test. The portions of mass passing and retained in sieves were recorded as M1 and gauged with an Elongation gauge. The mass of material retained on the gap between the pins of the Elongation gauge was recorded as M2. The Elongation Index of each portion was calculated as given in equation 3.4.

$$\text{Elongation Index (FI)} = \left(\frac{M_2}{M_1}\right) \times 100 \qquad 3.4$$

The Elongation index of the sample equals the summation of Elongation Indices of individual portions.

3.4.5.Aggregate Impact Value according to BS 812-112:1990 [33]

The resistance of the ballast aggregates to sudden shock load or impact was assessed according to BS 812-112:1990. More than 5 kg of size range 14-5 mm of graded ballast aggregate from Ethio-Djibouti Railway line were sieved in dry condition to obtain a portion which passing 14mm sieve and retained in 10mm sieve for subjecting to impact load. A prepared sample of aggregates of mass M1 was placed in a steel mould in three layers of approximately equal size and each layer is given 25 blows of tamping rod. The sample is subjected to 15 blows of 14 kg weight hammer falling freely from a height of 380 mm. The fine materials generated after 15 blows were recorded as M2. The Aggregate Impact Value was expressed as a percentage by weight of material passing 2.36 mm standard sieve as given in equation 3.5.

$$\text{Aggregate Impact Value (AIV)} = \left(\frac{M_2}{M_1}\right) \times 100 \qquad 3.5$$

3.4.6.Aggregate Crushing Value (ACV) according to BS 812-110:1990 [33]

The resistance of the ballast aggregates to crushing under gradually applied load was assessed according to BS 812-110:1990. More than 15 kg of size range 14-5 mm of graded ballast aggregate from Ethio-Djibouti Railway line were sieved in dry condition to obtain a portion which passing 14 mm sieve and retained in 10mm sieve for subjecting to crushing compressive load. A sample of aggregates was placed in a measuring cylinder in three equal layers and each layer is given 25 blows of tamping rod. The mass of the sample was measured and recorded as M1. The sample was transferred to the steel mold and a plunger was placed on top of the sample and leveled ready for crushing test. A compression load is applied at the top of the specimen and gradually increased to 400 kN within 10 minutes. The fine material generated after applying 400 kN was measured and recorded as M2. The Aggregate Crushing Value was

expressed as the percentage by weight of material passing 2.36 mm standard sieve as given in equation 3.6.

$$\text{Aggregate Crushing Value (ACV)} = \left(\frac{M_2}{M_1}\right) \times 100 \quad 3.6$$

3.4.7.Specific Gravity and Absorption of Aggregates according to BS812:Part 2:1975[35]

The coarse ballast aggregates from the Ethio-Djibouti Railway line of size range 40mm-5mm of 2kg were taken as samples for this test. Approximately 2kg of a test sample of aggregate was placed in an airtight container with fresh clean water for 24±0.5 hours. The saturated sample was removed from the container, surface dried by two clothes, then weighed and recorded as mass B. The saturated sample was placed in the basket mesh and weighed in water as mass C. Finally, the surface dried aggregates were placed in an oven for 24±0.5 hours. After the prescribed time the dried aggregates were removed, leave to cool to room temperature. The dried aggregates were weighed in air and recorded as mass A. Calculations were carried out as follow:

1. Relative Density on an oven-dry basis (in ton/m^3)

$$\rho_d = \frac{A}{B - C} \quad 3.7$$

2. Relative Density / Bulk Specific gravity on a saturated and surface-dry basis

$$\rho_s = \frac{B}{B - C} \quad 3.8$$

3. Apparent Relative Density (in ton/m^3)

$$\rho_a = \frac{A}{A - C} \quad 3.9$$

4. Water Absorption (in % of dry mass)

$$W_{abs} = \left(100 \times \frac{(B-A)}{A}\right) \quad 3.10$$

4. RESULTS AND DISCUSSIONS

4.1. Field Investigation

The study of ballast degradation on the field through visual inspection identified some areas with vegetation growth, surface fines, shoulder ballast missing, cobles on the main track, more degraded ballast sections as shown in figures 14-17.



Figure 14: The section along Adama-Miesso at K 229+207 with mud plain, and vegetations

Figure 14 depicts a section near a pedestrian crossing. There are numerous fines from foot stepping, and the entire ballast is covered in mud plain. The presence of the mud plain enhanced the growth of vegetation. This section poses a risk to passing trains because the lateral stability is reduced due to the presence of fines and mud, and in the event of heavy rain, the mud can flow over the rails, resulting in a train derailment. The section from Figure 15 was also photographed near a pedestrian crossing, and the ballast is heavily crushed with numerous surface fines. There is no mud plain, and vegetation growth is in its early stages. Figure 16 shows a section with missing shoulder ballast, which can also impair track stability and drainage. Figure 17 depicts cobles on the main track, which pose a risk to passing trains because they can become stuck to the axles.



Figure 15: The section along Adama-Miesso at K210+ 626 with surface fines and high degraded ballast.



Figure 16: The section along Adama-Miesso at K274+810 with missing shoulder ballast



Figure 17: The section along with Adama-Miesso at K314+529 heaved shoulders and cobles on the main track.

4.2. Ballast Gradation

Using the sample locations described in the materials and methods section, samples were collected in eight different locations, and the results of the sieve analyses to investigate ballast degradation are shown in Figures 18-19, and the PSD curves for as-built and design limits are shown in Figure 27 in the appendix. Figure 18 shows the PSD curve shifting above the as-built maximum value, while Figure 19 shows the PSD curve shifting below the as-built minimum value. To determine how far the PSD curves deviated from the as-built values, the percentage of ballast particle breakage and additional ballast particles are calculated using the Area Ratio Method, and the results are shown in Table 14, Figures 20(a)-(d) and in the appendix Figure 28-31. The Marsal Breakage Index, Bg, was calculated to evaluate the degradation of ballast aggregates, and the results are plotted in Figure 21. The effect of ballast degradation was determined by calculating the coefficients of permeability and uniformity, as illustrated in Figure 22.
Table 15 summarizes ballast degradation based on gradation change. Figures 23(a)-(d) show the comparison between the present gradations with the AREMA gradations.

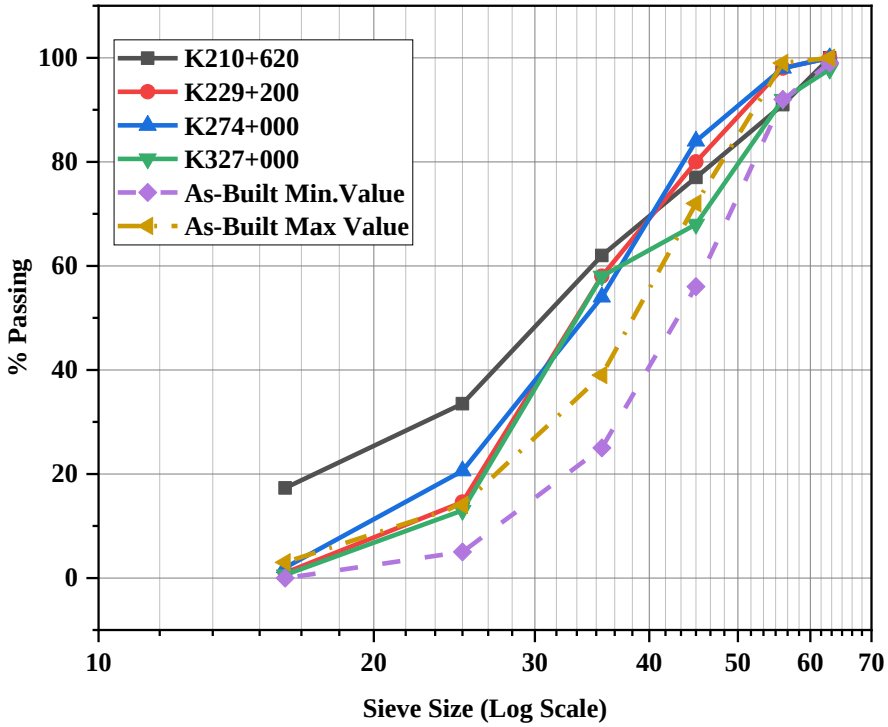


Figure 18: PSD curves with percentage passing above the as-built maximum value

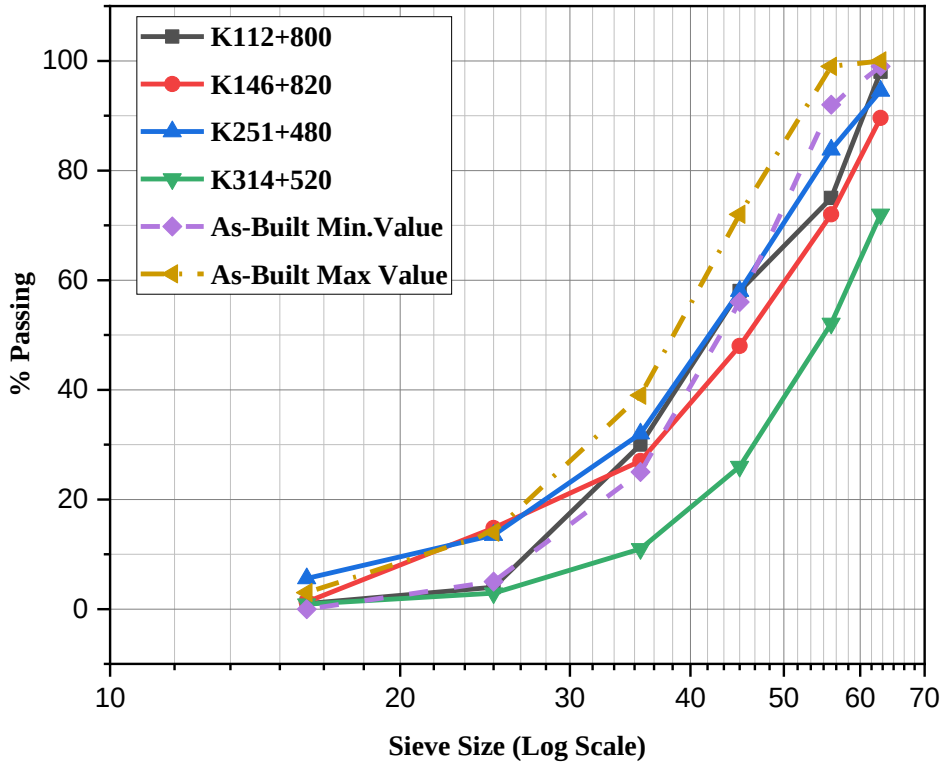


Figure 19: PSD curves with percentage passing below the as-built minimum value

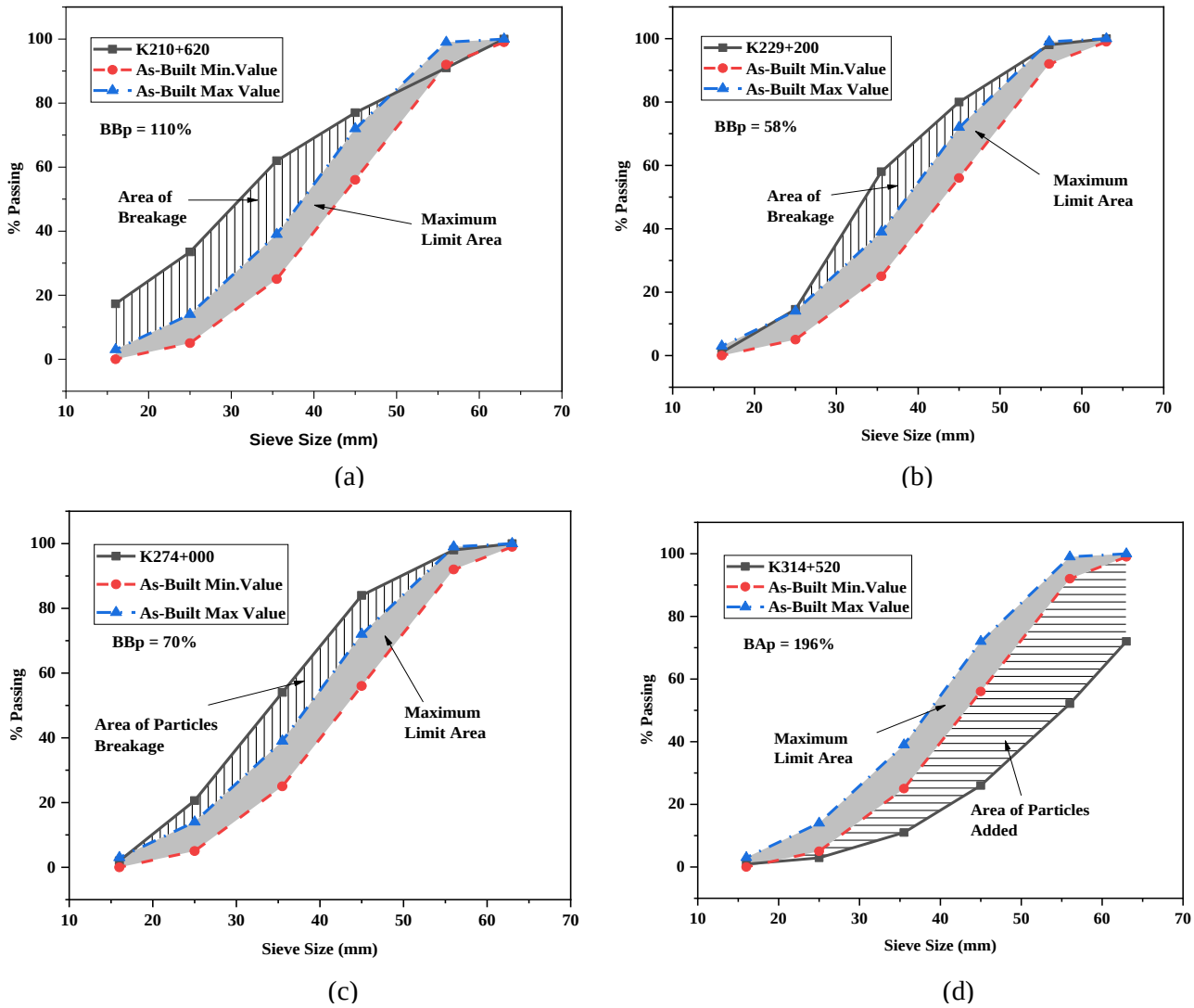


Figure 20: PSD Curves compared with the as-built limits

Table 14: Percentage (%) shift of PSD curves from the as-built values

Chainage	Ballast Breakage(BBp) (Above the as-built max. value)	Ballast Additional (Bap) (Below the as-built Min.Value)
K112+800		31
K146+820		61
K210+620	110	
K229+200	58	
K251+480	2.1	17
K274+000	70	
K314+520		196
K327+000	36	

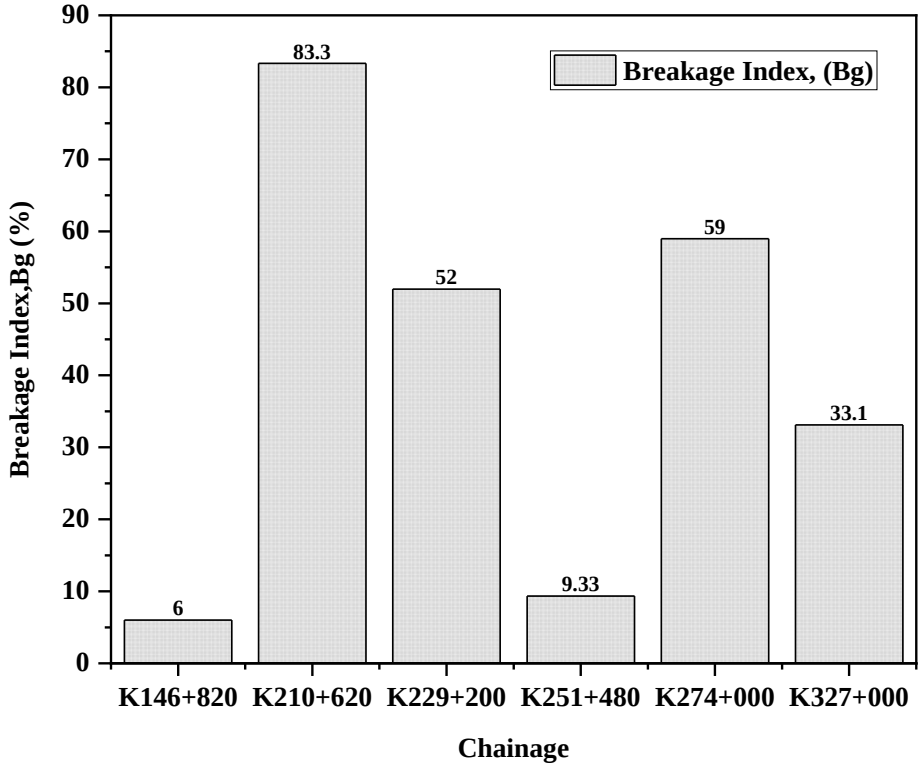


Figure 21: Ballast Breakage Index (Bg) of aggregates along Adama-Miesso Section

The gradations of ballast aggregates from each location deviate from the as-built limits used during construction, as demonstrated by the test results shown in Figures 18-19. Some gradations are higher than the as-built maximum limits, while others are lower than the as-built minimum limits. The percentage of ballast passing the standard sieves increased as the degradation progressed, and where the degradation is severe, the percentage passing is greater than the maximum design limit. If performed correctly, any ballast maintenance should keep the gradations within the limits. Without a proper investigation of the existing gradation in situ, the gradation curve is below the lower limits implies that the gradation is shifting to a broader range due to additional materials beyond the recommended design lower limits, Figure 27 appendix. As a result of the degradation and improper maintenance of ballast material, as well as the addition of incorrect proportions, the ballast layer functions are compromised. The drainage and storage functions should not be compromised in any design of the ballast layer. The results of the ballast grading are summarized in Table 15.

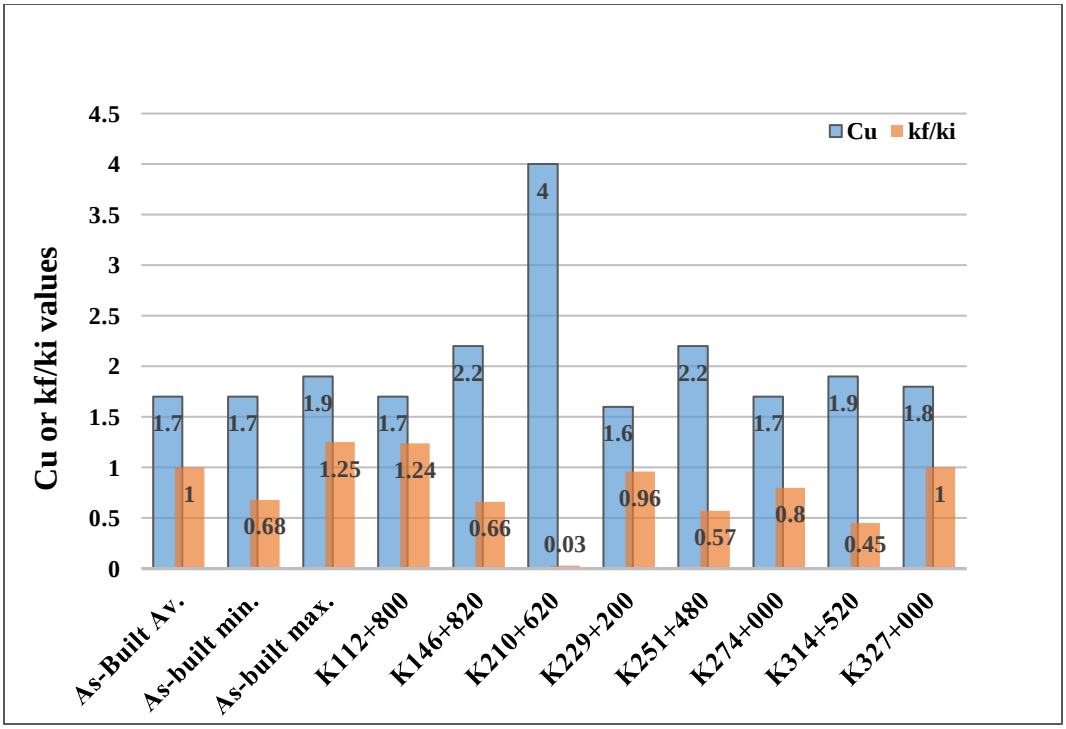


Figure 22: Coefficient of Uniformity Cu, and Permeability Factor, kf/ki of ballast

Following three years of operation, Figure 22 shows the effect of ballast degradation on the ballast layer's coefficient permeability. The fact that the coefficient of permeability decreases as the coefficient of uniformity increases implies that permeability is inversely proportional to the coefficient of uniformity, as expected. As Marsal's breakage (Bg) increases, the coefficient of uniformity increases, indicating that the material becomes more graded, as illustrated in Figure 21 and Figure 22.

Table 15: Gradations and observations from different locations

Location	Observations on gradations	Comments	Remarks
K112+800	Improper addition of material of size range 63-50 mm; cause a shift of PSD curve of 31 % below the as-built minimum value, Table 14. And Figure 28 The coefficient of uniformity, Cu, and permeability factor of about 1.7 and 1.24, respectively, Figure 22.	The gradation might be good for drainage and storage for fouling materials. The permeability factor increased by 24% when compared with the as-built average value.	The gradation Curve is within AREMA 24 except there is a small decrease of material passing 25-28mm standard sieve sizes, Figure 23 (a).

Location	Observations on gradations	Comments	Remarks
K146+820	Improper addition of materials of size range from 63-37.5mm standard sieve sizes; cause a shift of 61 % below the as-built minimum value, Table 14 and Figure 29. Particle Breakage Index, Bg is 6 %, Figure 21. The coefficient of uniformity, Cu, and permeability factor of about 2.2 and 0.66, respectively, Figure 22.	The gradation might be fair for drainage and storage of fouling material. The permeability factor decreased by 34% when compared with the as-built average value.	The gradation curve is within AREMA 24 Figure 23(a).
K210+620	There is severe degradation of material size range from 45-16 mm; cause a shift of PSD curve of 110 % above the as-built maximum value, Figure 20(a) and Table 14. Particle Breakage Index, Bg is 83.3 %, Figure 21. The coefficient of uniformity, Cu, and permeability factor of about 4 and 0.03, respectively, Figure 22.	The gradation might be poor for drainage as well as the storage for fouling materials. The permeability factor decreased by 97% when compared with the as-built average value.	The gradation Curve is within AREMA 25 except the is a slight increase of material passing 9.5-4.75 mm standard sieve sizes, Figure 23(b)
K229+200	There is severe degradation of material size range from 56-25 mm; cause a shift of PSD curve of 58 % above the as-built maximum value, Figure 20(b) and Table 14. Particle Breakage Index, Bg is 52 %, Figure 21. The coefficient of uniformity, Cu, and permeability factor of about 1.6 and 0.96, respectively, Figure 22	The gradation might be good for drainage and storage of fouling materials. The permeability factor decreased by 4% when compared with the as-built average value.	The gradation curve is within AREMA 24, Figure 23(a).

.

Location	Observations on gradations	Comments	Remarks
K251+480	Improper addition of material of size range 63 - 50 mm; cause a shift of PSD curve of 17 % below the as-built minimum value. There is a degradation of material of size range 25 - 16 mm; cause a shift of PSD curve of 2.1 % above the as-built maximum value, Table 14 and Figure 30. Particle Breakage Index, Bg is 9.3 %, Figure 21. The coefficient of uniformity, Cu, and permeability factor of about 2.2 and 0.57, respectively, Figure 22.	The gradation might be fair for drainage and storage of fouling material. The permeability factor decreased by 43% when compared with the as-built average value.	The gradation curve is within AREMA 24, Figure 23(a).
K274+000	There is severe degradation of material size range from 56-25 mm, cause a shift of PSD curve of 70 % above the as-built maximum value, Figure 20(c) and Table 14. Particle Breakage Index, Bg is 59 %, Figure 21. The coefficient of uniformity, Cu, and permeability factor of about 1.7 and 0.8, respectively, Figure 22.	The gradation might be fair for drainage and storage of fouling material. the permeability factor decreased by 20% when compared with the as-built average value.	The gradation curve is within AREMA 4A, Figure 23(d).
K314+520	Improper addition of material of size range 63-25 mm; cause a shift of PSD curve of 196 % below the as-built minimum Value, Figure 20(d) and Table 14. The coefficient of uniformity, Cu, and permeability factor, of about 1.9 and 0.45, respectively, Figure 22.	The gradation might be poor for drainage and storage of fouling material. The permeability factor decreased by 55% when compared with the as-built average value.	The gradation curve can not fit any of the broadly AREMA gradations Figure 23(c).

Location	Observations on gradations	Comments	Remarks
K327+000	There is a degradation of material of size range 35.5-16 mm; cause a shift of PSD curve of 36 % above the as-built maximum value, Table 14. and Figure 31. Particle Breakage Index, Bg is 33.1 %, Figure 21. The coefficient of uniformity, Cu, and permeability factor of about 1.8 and 0.73, respectively, Figure 22.	The gradation might be fair for drainage and storage of fouling material. The discharge factor decreased by 27 % when compared with the as-built average value.	The gradation curve is within AREMA 24, Figure 23(a).

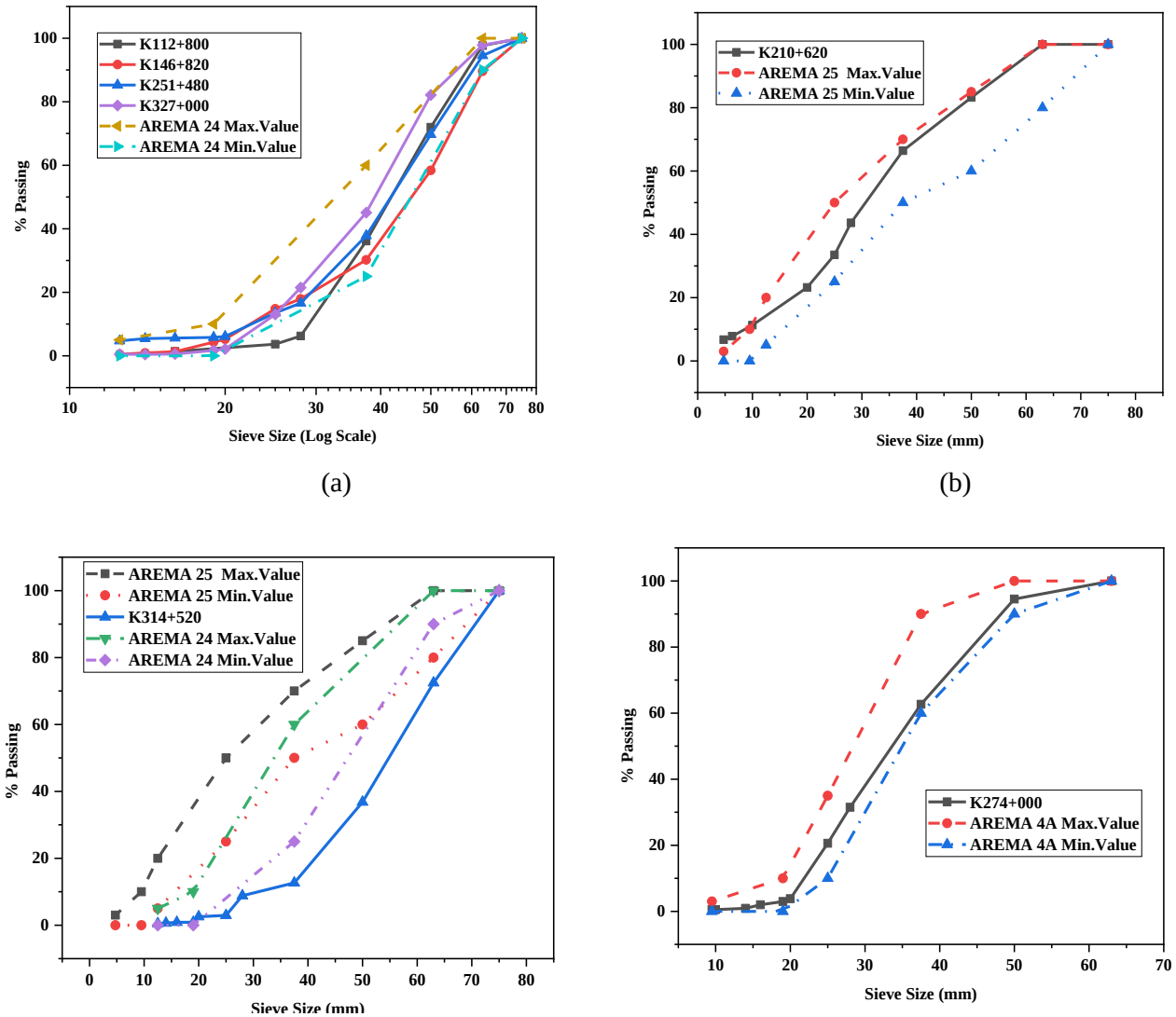


Figure 23: Comparison of PSD curves of ballast aggregates with AREMA gradations

4.3. Ballast Properties

The mechanical, shape, and physical properties of the samples were analyzed in the laboratory. These properties included Los Angeles Abrasion Value, Aggregate Impact Value, and Aggregate Crushing Value (Mechanical Properties), Elongation and Flakiness Indices (shape properties), and Specific Gravity, Abstraction, and Particle Fouling Index (Physical Properties).

4.3.1 Ballast Mechanical Properties

The results of laboratory tests conducted on the mechanical properties of samples collected at various locations are depicted in Figure 24. The highest and lowest LAAVs are found in ballasts at chainages

K274+000 and K146+820 (33 percent and 17 percent, respectively). Additionally, the highest and lowest AIV values are found for ballasts at chainages K229+200 and K327+000 (17 percent and 4 percent, respectively). For the ACV, however, the ballast appears to have a constant value of around 20% across all chainages. The mechanical properties of the ballast at the selected locations are listed in Table 16, along with the recommended limits specified in European, Australian, and AREMA standards. Except for the ballast at Chainage K274+000, all LAA values are less than the ASTM maximum value (30 percent). Additionally, the AIV and ACV are within the recommended ranges for all locations (22 percent EN 1097-2 and 25 percent AS, respectively).

Table 16: Ballast mechanical properties and the recommended values in standards

Chainage	LAAV	AIV	ACV
146+820	18	17	19
210+620	25	6	20
229+200	22	17	19
251+480	19	9	17
274+000	33	7	19
314+520	20	8	20
327+000	20	4	18
Adama	21	12	20
Recommendations	**Max 30% ASTM-C535-C131**	**<22% EN 1097-2**	**<25% AS**

ASTM = American Standard Test Method, EN = European AS = Australian Standard

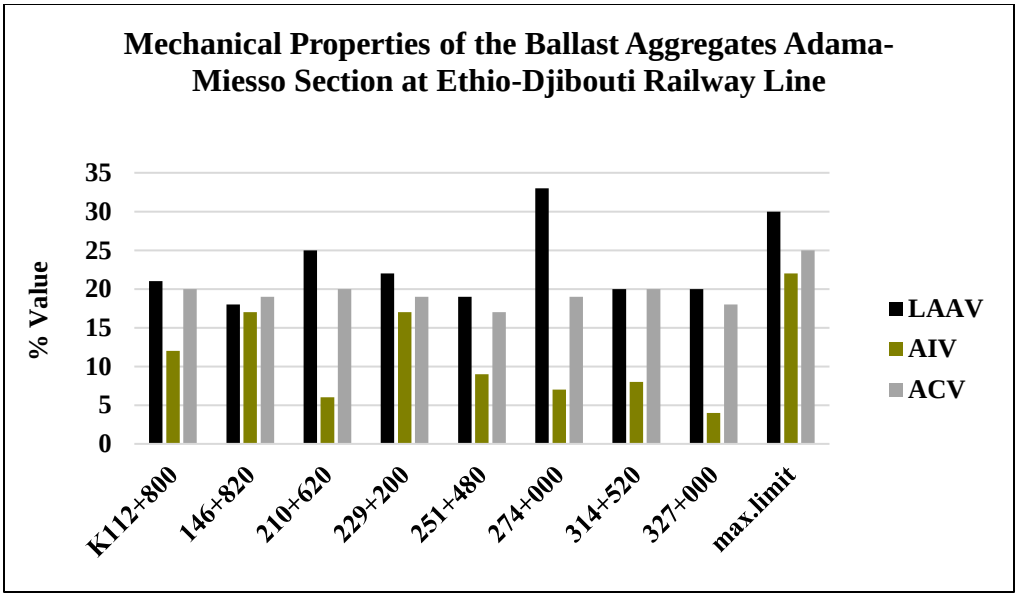


Figure 24: Mechanical properties of the ballast aggregates and recommended maximum limits

4.3.2. Ballast Shape Properties

The ballast shape properties (elongation and flakiness indices) were determined for chosen ballast samples to explore their form qualities; the findings are shown in Figure 25. Ballast at chainages K229 + 200 and K210 + 620 has the highest (43%) and lowest (11%) EI values, whereas ballast at chainages K314+520 and K210 + 620 has the highest (35%) and lowest (8%) FI values. According to the design specification, the recommended EI and FI values are 50%; thus, the ballast shape parameters at the selected places are within the recommended values.

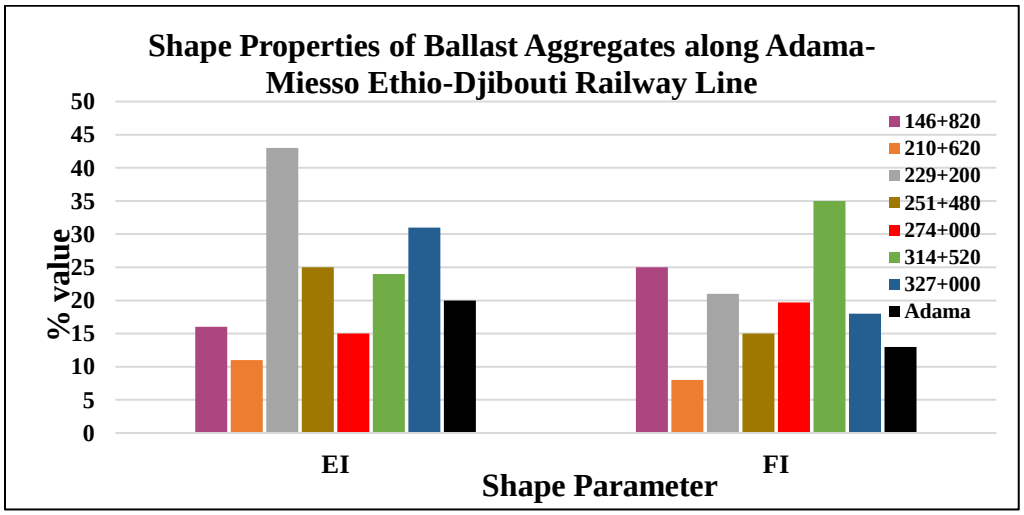


Figure 25: A Clustered Bar Chart Showing the Shape Properties of the Ballast at Different Locations

4.3.3 Ballast Physical Properties

The ballast physical qualities, including specific gravity, absorption, and particle size less than 0.075 mm sieve size were examined. As illustrated in Figure 26, the ballast SG ranges between approximately 2.4 and 2.8, reaching its highest and minimum values at chainages K314 + 520 and K146 + 820, respectively. Again, ballast materials with chainages K146 +820 and K327 + 000 exhibit the highest and lowest absorption values of 2.2 and 1.2 percent, respectively. Furthermore, for particles smaller than 0.075mm, ballast materials at chainages K210 + 620 and K229 + 200 had the highest and lowest values of around 2.3 percent and 0.3 percent, respectively.

As shown in Table 17, ballast materials with chainages K146 + 820 (2.4) and K274 + 000 (2.5) have SG values less than the recommended value (Min 2.6 ASTM-C127), while others have values within the recommended range. Additionally, only the ballast material at chainage K146 + 820 contains an amount of Abs (2.2 percent) that exceeds the permissible value (1-2 percent ASTM-C127), while the others are within the recommended range. And for Particles finer than 0.075mm, the ballast materials at chainages K210 + 620 and K251 + 480 have particle finer than 0.075 mm sieve size values (2.3 percent and 1.1 percent, respectively) that exceed the recommended value (Max 1 percent ASTM-C117), while the remaining values are within the recommendation.

Table 17: Ballast physical properties and the AREMA recommended values

Chainage	SG	Abs	P < 0.075 mm
112+800	2.6	1.8	0.6
146+820	2.4	2.2	0.4
210+620	2.6	1.9	2.3
229+200	2.6	1.6	0.3
251+480	2.7	1.3	1.1
274+000	2.5	1.8	0.9
314+520	2.8	1.4	0.4
327+000	2.7	1.2	0.4
Recommendations	**Min 2.6 t/m3 ASTM-C127**	**Max 1 - 2% ASTM-C127**	**Max 1% ASTM-C117**

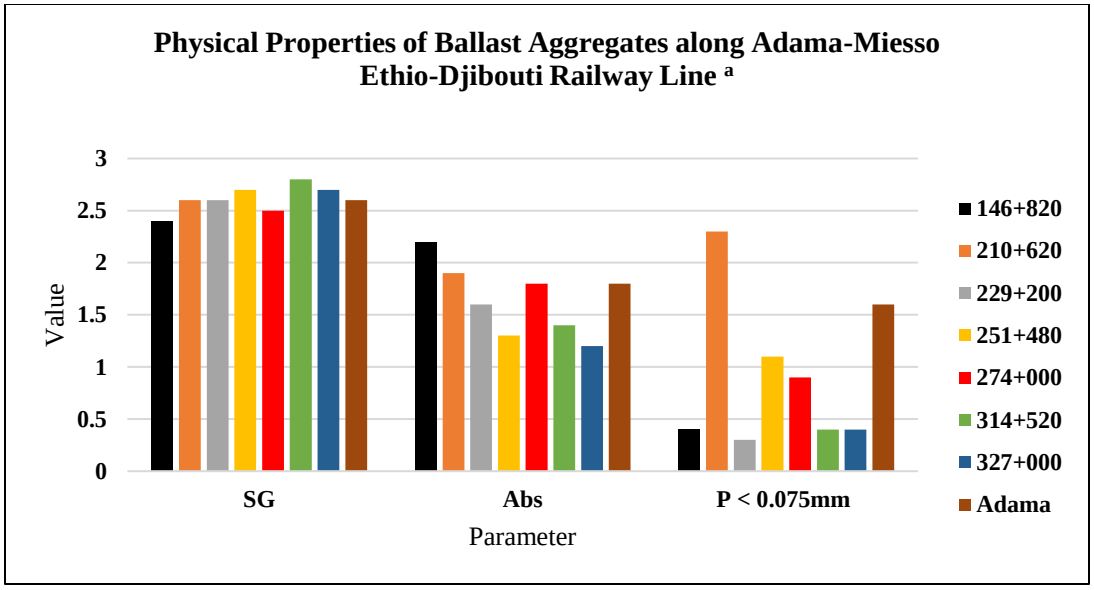


Figure 26: A Clustered Bar Chart Showing the Physical Properties of the Ballast at Different Locations

[a] = defines all the values are in percentage (%) except for the Specific Gravity, SG (t/m^3)

4.4. Summary of Result Findings

The results of the overall ballast degradation at the selected locations are summarized in Table 18 which contains the physical, shape, and mechanical properties' results and their comparisons with the recommendations in the standards.

Table 18: Summary of ballast properties degradation at the selected locations

Parameter/ Chainage	Mechanical			Shape		Physical		
	LAAV	AIV	ACV	EI	FI	SG	ABS	P < 0.075mm
112+800	*	*	*	*	*	*	*	*
146+820	*	*	*	*	*	**	**	*
210+620	*	*	*	*	*	*	*	**
229+200	*	*	*	*	*	*	*	*
251+480	*	*	*	*	*	*	*	**
274+000	**	*	*	*	*	**	*	*
314+520	*	*	*	*	*	*	*	*
327+000	*	*	*	*	*	*	*	*
112+800	*	*	*	*	*	*	*	*

** Defines that the results are within the recommendations in the standards*

*** Defines that the results are **NOT** within the recommendations in the standards*

CONCLUSIONS AND RECOMMENDATIONS

4.5. Conclusions

The following results have been reached regarding ballast degradation along the Adama-Miesso section of the Ethio-Djibouti Railway Line:

The study discovered that the most damaged sites are those around pedestrian crossings, where mud plain, dense vegetation, and surface fines were noted. Additionally, there are difficulties with ballast deficit, particularly in the shoulders, ballast depth loss, and shoulder portions heaving owing to track subsidence in some parts. Again, boulders are strewn across and between the sleepers.

Within three years of operation, there is significant deterioration of ballast, as shown by the PSD curves shifting above the as-built maximum values of 36-110 percent and Marsal Breakage Index of 33-83 percent. Improper ballast aggregate addition has been found, as indicated by PSD curves dropping below the as-built minimum value of 31-196 percent. The degrading process resulted in a significant reduction in the permeability of ballast of around 34-97 percent, as illustrated in Figure 22. The majority of ballast aggregates throughout the Adama-Miesso stretch are broadly graded and fall within AREMA 24-25, while others are even more broadly graded than AREMA 25, as illustrated in Figures 23(a)-(d).

Abrasion, crushing, and impact tests revealed that the resistance of the present ballast to abrasion, impact, and crushing is between 67 and 81%, 83 to 96%, and 80 to 83%, respectively. However, due to a lack of data on the As-Built values for the abrasion, crushing, and impact tests, an adequate judgment regarding whether these results varied from the initial values or not could be drawn. Additionally, when the values are compared to the recommendations in various standards, it can be concluded that the ballast is still capable of carrying the imposed loads only if a strong ballast matrix can be formed; however, field investigations and PSD analysis revealed that the ballast has degraded significantly over the last three years of operation, making it difficult to form a strong ballast matrix through aggregate interlocking. The aggregate interlock is critical because it provides lateral stability and the ability to withstand the transmission of significant train loads from the superstructure [36].

When compared to the as-built maximum values, Figure 25 and Table 19 in Appendices, the flaky and elongated particles rise from a maximum of 24 to 35 percent, and 22 to 43 percent, respectively. The flaky and elongated ballast particles disintegrate more rapidly.

Additionally, the study can conclude that the ballast stones are of normal weight because their average specific gravity and absorption rates are around 2.6 t/m3 and 1.7 percent, respectively, as shown in Table 17 and Figure 26.

4.6. Recommendations

The following recommendations are given in light of the primary objective, the field and laboratory research, and the conclusions:

• The report advises that the investigations be repeated using a full-scale triaxial test to model an in-situ ballast degradation trend to assess its carrying capacity.

• It is advised that pedestrians have adequate crossings, such as overpasses, to avoid being fined from foot stepping.

• For ballast fouling testing, the use of digitalized equipment such as Ground Penetration Radar in conjunction with sieve analysis is advised.

• The investigation indicates that the degradation tendency is significant, and thus maintenance is necessary.

• The study advises that when selecting ballast quarries, the parent rock's mechanical, physical, and chemical qualities be examined using procedures suggested by various railway standards. To effectively prevent the incidence of particle deterioration, it is necessary to assess the quality of crushed aggregate by measuring the strength of parent rock [37].

References

[1] M. Koohmishi and M. Palassi, “Effect of particle size distribution and subgrade condition on degradation of railway ballast under impact loads,” *Granul. Matter*, vol. 19, no. 3, 2017, doi: 10.1007/s10035-017-0747-0.

[2] D. Bassey, B. Ngene, I. Akinwumi, V. Akpan, and G. Bamigboye, “Ballast contamination mechanisms: A criterial review of characterisation and performance indicators,” *Infrastructures*, vol. 5, no. 11, pp. 1–24, 2020, doi: 10.3390/infrastructures5110094.

[3] B. Indraratna, W. Salim, and C. Rujikiatkamjorn, *Advanced rail geotechnology - Ballasted track*. 2011.

[4] I. Ferestade, P. Hosseini Tehrani, and R. Heidary, “Fracture toughness estimation of ballast stone used in Iranian railway,” *J. Rock Mech. Geotech. Eng.*, vol. 9, no. 5, pp. 892–899, 2017, doi: 10.1016/j.jrmge.2017.03.017.

[5] W. R. Interaction, “Track Engineering,” no. January, 2004.

[6] G. Q. Jing, Y. M. Ji, W. L. Qiang, and R. Zhang, “Experimental and Numerical Study on Ballast Flakiness and Elongation Index by Direct Shear Test,” *Int. J. Geomech.*, vol. 20, no. 10, p. 04020169, 2020, doi: 10.1061/(asce)gm.1943-5622.0001791.

[7] J. M. Sadeghi, J. A. Zakeri, and M. E. M. Najar, “Developing Track Ballast Characteristic Guideline In Order To Evaluate Its Performance,” *Int. J. Railw.*, vol. 9, no. 2, pp. 27–35, 2016, doi: 10.7782/ijr.2016.9.2.027.

[8] Y. Liu, R. Gao, and J. Chen, “A new DEM model to simulate the abrasion behavior of irregularly - shaped coarse granular aggregates,” *Granul. Matter*, pp. 1–16, 2021, doi: 10.1007/s10035-021-01130-5.

[9] D. Ionescu, 2004, [online]. available: https://www.researchgate.net/publication/30389573_Evaluation_of_the_engineering_behaviour_of_railway_ballast.

[10] B. Indraratna and W. Salim, “Mechanics of Ballasted Rail Tracks: A Geotechnical Perspective.” p. 226, 2005.

[11] T. R. Sussmann, M. Ruel, and S. M. Chrismer, “Source of ballast fouling and influence considerations for condition assessment criteria,” *Transp. Res. Rec.*, no. 2289, pp. 87–94, 2012, doi: 10.3141/2289-12.

[12] T. C. Abadi, “Effect of Sleeper and Ballast Interventions on Rail Track Performance,” no. January,

p. 264, 2015, [online]. available: https://eprints.soton.ac.uk/id/eprint/388080.

[13] A. Y. Alemu, "Survey of Railway Ballast Selection and Aspects of Modelling Techniques," *Div. Highw. Railw. Eng. Div. Highw. Railw. Eng. Dep.*, pp. 1–61, 2011, [Online]. Available: http://urn.kb.se/resolve?urn=urn:nbn:se:kth:diva-87466.

[14] G. P. Raymond, "Research on Railroad Ballast Specification and Evaluation.," *Transp. Res. Rec.*, pp. 1–8, 1985.

[15] J. Kim, B. S. Park, S. I. Woo, and Y. T. Choi, "Evaluation of ballasted-track condition based on aggregate-shape characterization," *Constr. Build. Mater.*, vol. 232, p. 117082, 2020, doi: 10.1016/j.conbuildmat.2019.117082.

[16] B. Indraratna, "1st Ralph Proctor Lecture of ISSMGE. Railroad performance with special reference to ballast and substructure characteristics.," *Transp. Geotech.*, vol. 7, pp. 74–114, 2016, doi: 10.1016/j.trgeo.2016.05.002.

[17] F. Group, *Railway Geotechnics*, 1st Editio. CRC Press, 2016.

[18] R. P. P. D, "Report # MATC-KU : 465 Final Report Properties of Fouled Railroad Ballast (Phase 1)," p. 55, 2012.

[19] D. Ionescu, "Ballast Degradation and Measurement of Ballast Fouling," *7th Railw. Eng. Proc.*, no. July 2004, p. p.169-180, 2004.

[20] B. B. O. Hardin, "Hardin1985.Pdf," *J. Geotech. Eng.*, vol. Ill, no. 10, pp. 1177–1192, 1985.

[21] B. Indraratna, J. Lackenby, and D. Christie, "Effect of confining pressure on the degradation of ballast under cyclic loading," *Géotechnique*, vol. 55, no. 4, pp. 325–328, 2005, doi: 10.1680/geot.55.4.325.65490.

[22] B. Indraratna, H. Khabbaz, W. Salim, and D. Christie, "Geotechnical properties of ballast and the role of geosynthetics in rail track stabilisation," *Gr. Improv.*, vol. 10, no. 3, pp. 91–101, 2006, doi: 10.1680/grim.2006.10.3.91.

[23] B. Indraratna, Y. Sun, and S. Nimbalkar, "Laboratory Assessment of the Role of Particle Size Distribution on the Deformation and Degradation of Ballast under Cyclic Loading," *J. Geotech. Geoenvironmental Eng.*, vol. 142, no. 7, p. 04016016, 2016, doi: 10.1061/(asce)gt.1943-5606.0001463.

[24] K. M. Scanlan, *Evaluating degraded ballast and track geometry variability along a Canadian freight railroad through ballast maintenance records and ground-penetrating radar*. 2018.

[25] P. V. Lade, J. A. Yamamuro, and P. A. Bopp, "Closure to 'Significance of Particle Crushing in Granular Materials' by Poul V. Lade, Jerry A. Yamamuro, and Paul A. Bopp," *J. Geotech.*

Geoenvironmental Eng., vol. 123, no. 9, pp. 889–890, 1997, doi: 10.1061/(asce)1090-0241(1997)123:9(889).

[26] E. M. Onur, "Predicting the Permeability of Sandy Soils From," p. 123, 2014.

[27] M. Moaveni, Y. Qian, I. I. A. Qamhia, E. Tutumluer, C. Basye, and D. Li, "Morphological characterization of railroad ballast degradation trends in the field and laboratory," *Transp. Res. Rec.*, vol. 2545, pp. 89–99, 2016, doi: 10.3141/2545-10.

[28] X. Bian, K. Shi, W. Li, X. Luo, E. Tutumluer, and Y. Chen, "Quantification of Railway Ballast Degradation by Abrasion Testing and Computer-Aided Morphology Analysis," *J. Mater. Civ. Eng.*, vol. 33, no. 1, p. 04020411, 2021, doi: 10.1061/(asce)mt.1943-5533.0003519.

[29] Y. Guo, V. Markine, J. Song, and G. Jing, "Ballast degradation: Effect of particle size and shape using Los Angeles Abrasion test and image analysis," *Constr. Build. Mater.*, vol. 169, pp. 414–424, 2018, doi: 10.1016/j.conbuildmat.2018.02.170.

[30] "Standard Practice for Reducing Samples of Aggregate to Testing Size 1," *Astm C 702 - 9*, vol. 04, no. Reapproved, pp. 700–703, 2003.

[31] ASTM International, "C117-95. Standard Test Method for Materials Finer than 75-μm (No. 200) Sieve in Mineral," *Annu. B. ASTM Stand.*, vol. 04, no. 200, p. 4, 1995.

[32] B. Statements and T. Size, "Standard Test Method for Sieve Analysis of Fine and Coarse Aggregates 1," vol. i, no. 200, pp. 1–5, 2007.

[33] L. Copy, A. Koksal, and U. Copy, "British Standard Testing aggregates," no. December, 2002.

[34] BS 812-105.2, "Testing aggregates-Methods for determination of particle shape-Section 105.2 Elongation index of coarse aggregate," *Annu. B. BS Stand.*, no. January, 1990.

[35] T 85, "Specific Gravity of Coarse Aggregate," *Aashto*, pp. 1–8, 2012.

[36] H. Boler, Y. Qian, and E. Tutumluen, "Influence of size and shape properties of railroad ballast on aggregate packing statistical analysis," *Transp. Res. Rec.*, vol. 2448, no. December, pp. 94–104, 2014, doi: 10.3141/2448-12.

[37] M. Koohmishi, "Assessment of strength of individual ballast aggregate by conducting point load test and establishment of classification method," *Int. J. Rock Mech. Min. Sci.*, vol. 141, no. March, p. 104711, 2021, doi: 10.1016/j.ijrmms.2021.104711.

Appendices

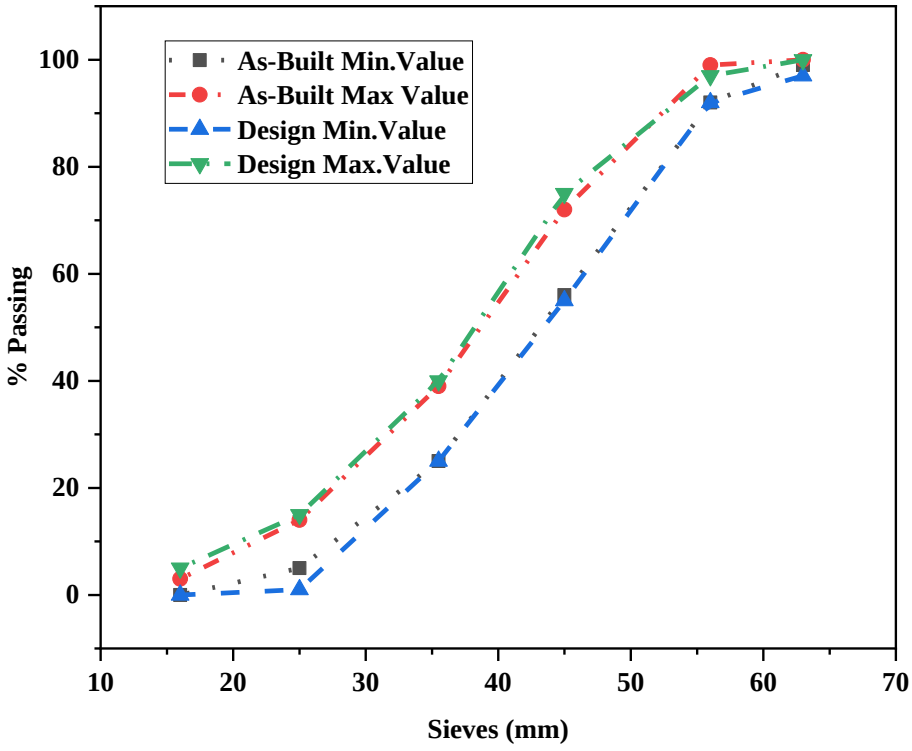


Figure 27: PSD curves of as-built compared with the design limits

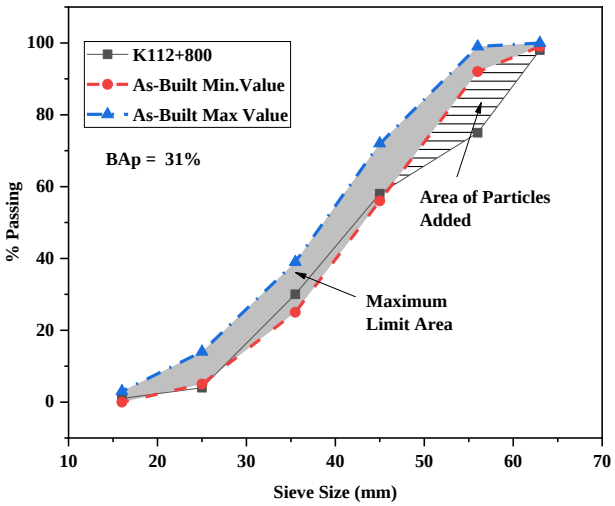


Figure 28: PSD curve at K112+800 section compared with the as-built limits

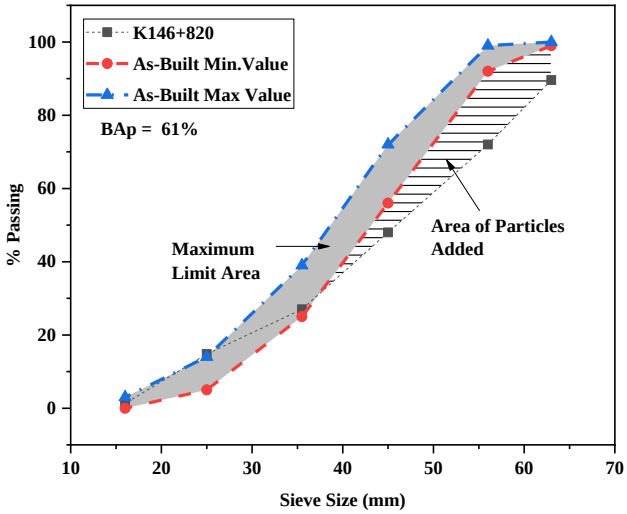


Figure 29: PSD curve at chainage K146+820 compared with the as-built limits

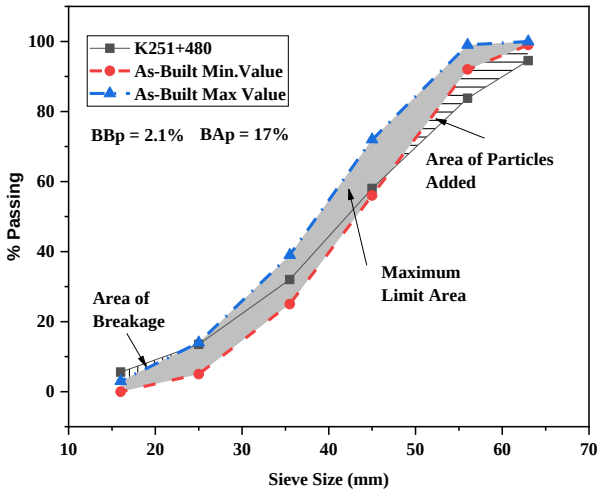


Figure 30: PSD curve at chainage K251+480 compared with the as-built limits

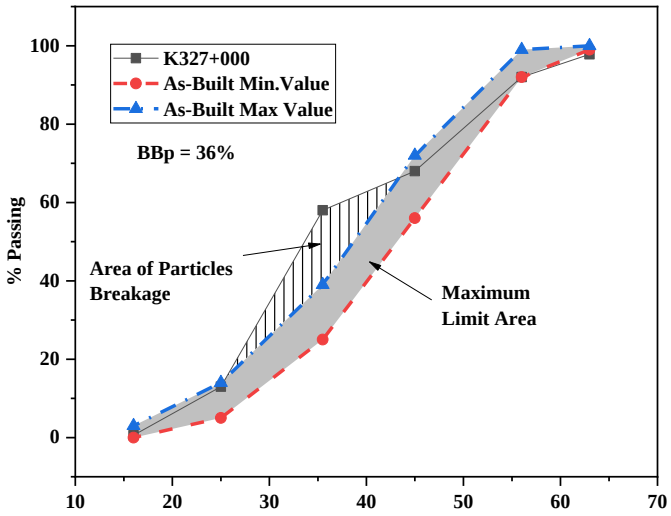


Figure 31: PSD Curves at Chainage K327+000 Compared with the as-built limits

Table 19: As-Built Parametric Values and Standard Specification Values

Specifications		Elongation Index	Flakiness Index	Clay lump and impurity content	Powder content of particles size < 0.1mm (%)
Standard	Minimum	0	0	0	0
	Maximum	50	51	0.5	1
As-Built	Average	19	17	0.3	0.7
	Minimum	16	14	0.1	0.4
	Maximum	22	24	0.4	0.9

Gradation	Sieve Size (mm)		16	25	35.5	45	56	63
% Passing	Standard	Minimum	0	5	25	55	92	97
		maximum	5	15	40	75	97	100
	As-Built	Average	1	9	32	65	93	100
		Minimum	0	5	25	56	92	99
		Maximum	3	14	39	72	99	100

Table 20: Current Insitu Ballast Aggregate Gradations

Sieve Size(mm)	% Passing							
	Adama	K146+820	K210+620	K229+200	K251+480	K274+000	K314+520	K327+000
63	98	89.6	100	100	94.5	100	72	97.8
56	75	72	91	98	83.8	98	52.1	92
45	58	48	77	80	58	84	26	68
35.5	30	27	62	58	32	54	11	58
25	4	14.8	33.5	14.6	13.5	20.6	2.9	13
16	1	1.3	17.3	1	5.6	2	0.9	0.6

Table 21: Calculation of Marsal Breakage ratio, B_g.

Sieve Size(mm)	Adama	K146+820	K210+620	K229+200	K251+480	K274+000	K314+520	K327+000
63	-2	-10	0	0	-5	0	-28	-2
56	-18	-21	-2	5	-9	5	-41	-1
45	-7	-17	12	15	-7	19	-39	3
35.5	-2	-5	30	26	0	22	-21	26
25	-5	6	24	5	4	11	-6	4
16	0	0	16	0	5	1	0	0
Breakage Ratio, Bg	0	6	83	52	9	59	0	33

3. Aggregate Crushing Value	
Chainage	**210+620**
Mass of dry Sample (g)	1748.5
Loading force kN	400
Loading time (minutes)	10
Mass of material passing 2.36mm sieve after crushing	341.8
ACV(%)	**20**

2. Los Angeles Abrasion Value Test	
Chainage	**210+620**
Grade	**2**
Mass of Dry Sample	10103.3
Mass of 12 steel balls(g)	5000
No.of revolutions	1000
Material finer than 1.7mm (g)	2557.3
LAAV(%)	**25**

Table 22: Ballast aggregates characteristics; D_{10}, D_{30}, D_{50}, D_{60}, k, k_f/k_i, C_u, and C_c

	Particle Size(mm)					**X-Intercept**	**Permeability**	**Permeability Factor**	C_u	C_c
	D_{10}	D_{30}	D_{50}	D_{60}	Dmax	$(5D_{10}-D_{50})/4$	k (m/day)	kf/ki		
Adama	27.3	35.5	42.3	46.1	56	23.55	861	1.24	1.7	1.0
K146+820	22.64	37.82	45.8	50.69	63	16.85	457	0.66	2.2	1.2
K210+620	8.7	23.3	30.9	34.8	45	3.15	21	0.03	4	1.8
K229+200	23.3	37	33.4	36.8	45	20.78	665	0.96	1.6	1.6
K251+480	20.97	34.3	42	46.2	56	15.71	397	0.57	2.2	1.2
K274+000	21.9	27.9	34.1	36.6	45	18.85	552	0.80	1.7	1.0
K314+520	21.9	46.6	55.1	58.5	63	13.6	313	0.45	1.9	1.7
K327+000	23.7	31.3	33.7	42.5	45	21.2	692	1.00	1.8	1.0
As-Built Av. Value	25	34.5	40.7	42.7	45	21.08	693	1.00	1.7	1.1
Design Max.Value	28.9	37.1	43.5	45	45	25.25	987	1.42	2	1.2
Design Min.Value	20.1	31.3	38.2	40.9	45	15.58	387	0.56	1.6	1.1
Definitions										
$k=1.5046*(I_o+0.025(D_{50}-D_{10}))^2$ [26]										
Io=X-Intercept of the slope of the line formed by D_{50} and D_{10} of the grain-size distribution curve (mm)										
$C_u=D_{60}/D_{10}$										
$C_c=D_{30}^2/(D_{10}*D_{60})$										
k_i=693 m/day										



(a)Sieve Analysis of Ballast Aggregates



(b)Ballast Aggregates Contain Fines due to Abrasion and Wear



(c) Flackiness Index Test



(d) Elongation Index Test



(e) Aggregate Impact Value Test



(f) Aggregate Crushing Value Test



(g) Specific Gravity and Absorption Test

Figure 32: Test methods for mechanical and physical properties